# Gold nanoprobes for theranostics

Gold nanoprobes have become attractive diagnostic and therapeutic agents in medicine and life sciences research owing to their reproducible synthesis with atomic level precision, unique physical and chemical properties, versatility of their morphologies, flexibility in functionalization, ease of targeting, efficiency in drug delivery and opportunities for multimodal therapy. This review highlights some of the recent advances and the potential for gold nanoprobes in theranostics.

**KEYWORDS: diagnostics ■ gold nanoparticles ■ imaging ■ therapeutics ■ toxicity**

**Balaji Panchapakesan[1], Brittany Book-Newell[2], Palaniappan Sethu[3], Madhusudhana Rao[4] & Joseph Irudayaraj*[2]**

*[1]Department of Mechanical Engineering, Small Systems Laboratory, University of Louisville, Louisville, KY 40292, USA*
*[2]Agricultural & Biological Engineering, Bindley Bioscience Center & Birck Nanotechnology Center, Purdue University, 225 S. University Street, West Lafayette, IN 47907-2093, USA*
*[3]Department of Bioengineering, University of Louisville, Louisville, KY 40292, USA*
*[4]Center for Cellular & Molecular Biology, Hyderabad, 500007, India*
**Author for correspondence: josephi@purdue.edu*

## What are gold nanoprobes?

Gold nanoprobes (GNPs) are nanometer scale particles made of gold in varying shapes and sizes. Typical nanoprobes take the form of spheres, rods, shells, stars, cages, crescents, boxes and prisms with sizes ranging from 2 to 500 nm. Most probes used in biomedical and life sciences applications lie in the range between 10 and 100 nm. Nanoprobes have been shown to function as effective contrast agents for imaging and photothermal therapy, and as drug delivery vehicles for targeted therapeutics. The ease of fabrication, chemical stability, multifunctionality and biocompatibility makes GNPs highly attractive for diagnostics and therapy.

## Background

Theranostics is the term coined to define the fusion of therapeutics and diagnostics. Theranostics focuses on the integration of information from a diverse set of biomarkers to create pharmaceutical formulations for a targeted subpopulation where the drug can display greater therapeutic efficacy and less toxicity [1,2]. Theranostics encompasses a wide range of subjects, including personalized medicine, bioinformatics, proteomics, genomics, pharmacogenomics and molecular imaging to develop efficient new targeted therapies with adequate benefit/risk to patients and a better molecular understanding of how to optimize drug selection. Figure 1 presents the cycle involved in biomarker discovery emanating from population-based studies, classification of a clinical phenotype and bioinformatics to predict biomarkers in a given subpopulation. From biomarker discovery to delivery of theranostics, nanotechnology can play a vital role in its ability to deliver diagnostic sensors and therapeutic formulations. Nanotechnology encompasses the creation and utilization of materials at the level of atoms, molecules, and supramolecular structures. Unique size-dependent electronic, optical, thermal and mechanical properties of nanomaterials are being exploited today in diverse areas ranging from computer chips to biology and medicine. The high surface area:volume ratio renders nanoparticles with the ability to functionalize with surface moieties that can be used to target specific sites, sequester proteins or even silence a gene inside a living cell. Many different types of nanoparticles including, gold nanorods (GNRs), carbon nanotubes and silicon nanowires have been proposed, synthesized and their physical properties have been investigated in different applications depending on their size and shape. Gold nanostructures in this context are unique due to their chemical inertness, nontoxicity and ease of surface functionalization with different molecular structures such as thiols, amines, nitrates and phosphines to create active sensors and formulations that can interact with biological materials both *in vitro* and *in vivo*.

Gold is a byproduct of supernova nucleosynthesis and has fascinated human beings for thousands of years. It has been described in the Egyptian texts as early as 2600 BC. The fabrication of gold nanoparticles has been documented as early as the 4th century when Roman craftsmen used the particles to create stained glass and pottery. Michael Faraday's fascination with ruby gold and his methods to synthesize reproducible and stable gold suspensions with a particle size between 6 ± 2 nm and his investigations into the physical properties of gold colloids may

future medicine part of fsg

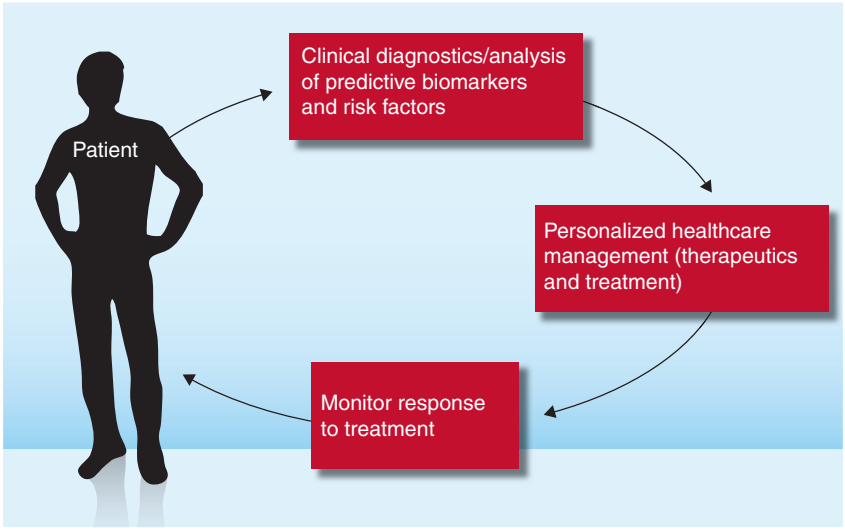


**Figure 1. Delivery of theranostics.**

have been the starting point of modern nanotechnology [3]. Over the years many different shapes and sizes of gold nanostructures have been synthesized. Interest in gold nanoparticles has increased almost exponentially in the last 10 years in biological engineering (Figure 2). Today gold nanoparticles as plasmonic nanostructures are used as sensors and drug delivery agents in applications such as detection of pathogens, photothermal transducers for minimally invasive therapy, the treatment of blood clotting related disorders, and contrast agents in imaging and in therapeutic formulations to name a few. The utilization of nanoparticles such as gold for theranostic purposes for simultaneous imaging, diagnosis and therapy in one step with the ability to monitor treatment efficacy is expected to offer a variety of options in nanomedicine.

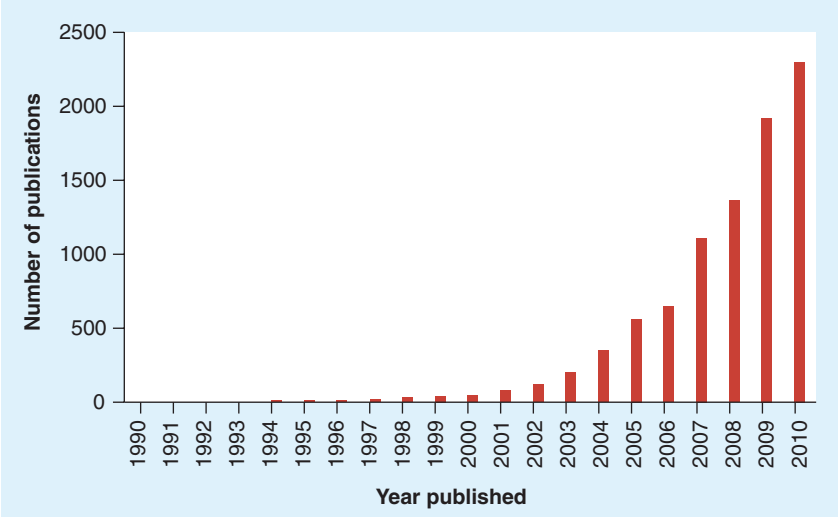


**Figure 2. Gold nanoprobe research trends in biological engineering.**

In this review we attempt to provide our perspective on the use of gold nanoprobes in diagnostics and therapeutics with an emphasis on cancer. The synthesis and morphology of different types of gold nanoprobes and their size ranges are dealt with in detail. Optical absorption and scattering cross-sections of different types of gold nanoprobes are compared against conventional organic dyes (Table 1) and their utility in sensing and molecular imaging is discussed. The electron thermalization events in gold nanoprobes leading to their application in photothermal and radiofrequency (RF) therapy to kill cancer cells are discussed. While the physical properties of gold are intrinsic in nature, we also showcase and discuss biologically relevant extrinsic factors for successful targeting, namely surface functionalization of nanoprobes, molecular targeting and cellular internalization that can enable drug and gene delivery. Finally, we look into the limited data on the biological toxicity of GNPs. The review concludes with potential futuristic insights and their relevance in detection and treatment.

## Synthesis, morphology & properties of GNPs

GNPs come in different shapes and sizes. Control over shape, size and chemical composition of GNPs itself is a challenging area of research that eventually determines the surface functionality and activity. The most common shapes are spherical particles, rods, shells, cages, prisms and stars. Figure 3A presents the transmission electron microscopy images of spheres, rods and stars, and their optical absorbance (Figure 3B). Spectral comparison in Figure 3C shows their utility in surface-enhanced Raman spectroscopy (SERS). The following paragraphs review the synthesis and physical properties of GNPs.

Stable and spherical gold nanoparticles ranging between 10 and 100 nm can be formed in a number of ways. The classic method is gold reduction from $HAuCl_4$ via citrate at 100°C, and was developed in the early 1950s by Turkevich *et al.* [4–6]. By varying the concentration of the gold versus citrate, one can tune the size of the gold nanoparticles synthesized. Recently, Turkevich's method has been revisited and compared with its variants, namely UV-initiated reduction and ascorbate reduction [7,8]. Results showed that control of the simple Turkevich process by the reduction conditions is sufficient to define particles' shape and size in a wide interval. The UV-initiated particle growth in contrast resulted in more spherical-like particles even at larger sizes. Ascorbate reduction

ensured the best spherical definition of the particles. Extensive networks of gold nanowires were also formed as a transient intermediate in the citrate reduction method [7]. These gold nanowires were shown to exhibit nonlinear optical properties and also contributed to the dark appearance of the reaction solution before it turned ruby-red. Another popular fabrication method is called the 'Brust synthesis' developed in 1994 by Brust and Schiffrin *et al.* [9,10]. In this method, organic liquids such as toluene, reducing agents such as $NaBH_4$ and tetraoctylammonium bromide (TOAB) are used to synthesize gold colloid particles from $HAuCl_4$. TOAB, a phase transfer agent, acts as a stabilizer; however, it does not form a strong bond with gold, which may cause particle aggregation after a few weeks. Another more recently developed method by Perrault *et al.* uses hydroquinone in an aqueous environment to grow nanoparticles of various sizes by the reduction of $HAuCl_4$. This method can produce monodispersed gold nanospheres in sizes ranging from 50 to 200 nm [11].

A simple but versatile variation of the spherical gold nanoparticle is the nanorod [12]. GNRs can be synthesized with different aspect ratios and are particularly useful in imaging, because they produce strong and tunable plasmonic resonance properties in the red to near-infrared (NIR) region of the electromagnetic spectrum [13–16]. GNRs and silver nanorods can be prepared using electrochemical and seed-mediated growth methods [12,17–20]. In the electrochemical method, a platinum cathode and gold anode are immersed in an electrolytic solution in an ultrasonic bath at 36°C containing hexadecyltrimethylammonium bromide and a small amount of hydrophobic cosurfactant tetradodecylammonium bromide. The surfactant serves to stabilize and prevent the aggregation of nanoparticles. Controlled electrolysis at 3 mA for 30 min leads to the formation of nanorods. In the seed-mediated approach, citrate-capped gold nanoparticle seeds with a diameter of 3.5 nm are used for the nucleation and reduction of gold salt in the presence of cetyl trimethyl ammonium bromide and ascorbic acid. This produced nanorods with a 4.6 ± 1 aspect ratio. It was found that addition of silver nitrate enhanced the formation and aspect ratio of nanorods. While the initial yield was poor using this method (~4%), nanorods of high yield (90%) using seed-mediated growth have been reported by slightly increasing the pH of the solution [21].

Gold-coated dielectric nanoparticles are called gold nanoshells [22–24]. This configuration of a dielectric core coated with a metal nanoshell occur naturally in the growth of Au-$Au_2S$ nanoparticles. Silica-coated gold nanoshells are produced by growing silica nanoparticles

**Table 1. Gold nanoprobes: optical properties and applications.**

| Gold nanoprobes | Optical property | Application |
|---|---|---|
| Nanospheres | $C_{abs} = 2.93 \times 10^{-15}$ ($m^2$), at $\lambda_{max}$ =528 nm, for 40 nm particle diameter $C_{sca}$ =$1.23 \times 10^{-14}$ ($m^2$) at 560 nm, for 80 nm particle diameter [51] | Contrast agents in OCT, photothermal heating, cellular uptake |
| Nanoshells | $C_{abs} = 5 \times 10^{-14}$ ($m^2$) and $C_{sca}$ =$3.25 \times 10^{-14}$ ($m^2$) at $\lambda_{max}$ =892 nm, for 140 nm particle diameter [52] | Contrast agents in OCT, photothermal heating, TPS and cellular uptake |
| Nanorods | $C_{abs} = 1.97 \times 10^{-14}$ ($m^2$) and $C_{sca} = 1.07 \times 10^{-14}$ ($m^2$) at $\lambda_{max}$ =842 nm, for effective radius = 21.86 nm and aspect ratio R = 3.9 [51] | Contrast agents in OCT, photothermal heating, TPS and cellular uptake |
| Nanocages | $C_{abs} = 7.3 \times 10^{-15}$ ($m^2$), $C_{sca}$ =$0.8 \times 10^{-15}$ ($m^2$) at $\lambda_{max}$ =825 nm, for 36 nm particle [42] | Contrast agents in OCT, photothermal heating, TPS, cellular uptake |
| Nanostars | SERS enhancement factor of $5 \times 10^3$ averaged over the 52 nm nanostars for 633 nm excitation [38] | SERS, plasmonic transducers for biosensing |
| Conventional NIR indocyanine green | $C_{abs}$ =$1.66 \times 10^{-20}$ ($m^2$) at $\lambda_{max}$ =778 nm, $\varepsilon = 1.08 \times 10^4$ $M^{-1}cm^{-1}$ at 778 nm [51] | Conventional organic dyes used in imaging |
| Rhodamine 6G | $\varepsilon = 1.16 \times 10^5$ $M^{-1}cm^{-1}$ at 530 nm [51] | Conventional strongly absorbing organic dye used in imaging |

*$C_{abs}$: Absorption cross section; $C_{sca}$: Scattering cross section; ε: Molar extinction coefficient; NIR: Near infrared; OCT: Optical coherence tomography; SERS: Surface-enhanced Raman spectroscopy; TPS: Two-photon scattering.*

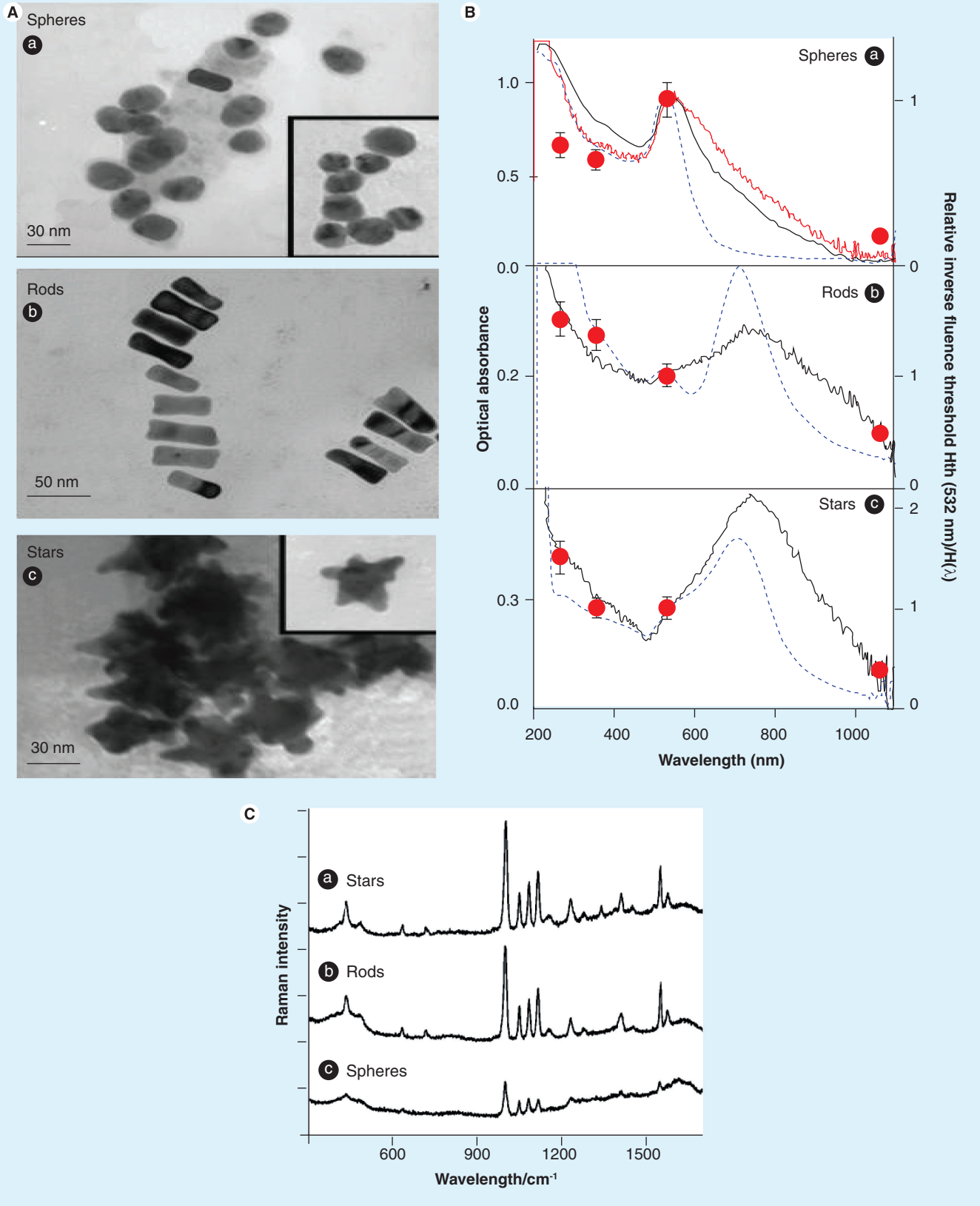


**Figure 3. Physical properties of some select nanoprobes. (A)** Transmission electron microscopy images of gold nanoprobes: **(a)** spheres; **(b)** rods; and **(c)** stars, **(B)** optical absorbance versus wavelength for the three different morphologies of gold nanoprobes and **(C)** SERS spectra comparison of 2 MPy absorbed on: **(a)** nanostars (140 nm), **(b)** nanorods (65 × 30 nm) and **(c)** nanospheres (150 nm). Reproduced with permissions from [33,227].

and coating then with a layer of gold to form a core–shell structure. Reduction of tetraethylorthosilicate in ammonium hydroxide and ethanol produces silica nanoparticles of 40–120 nm in diameter. Next, colloidal gold nanoparticles are used as seeds to stick to the silica nanoparticles, which form a discontinuous gold layer. Further gold is added by reducing $HAuCl_4$ in the presence of potassium carbonate and formaldehyde. By tuning the diameter of the core and thickness of the shell, one can tune the optical properties of the nanoshells to a wide range of wavelengths, including the 'water window', which is the IR range of the electromagnetic spectrum [25]. Gold nanoshells possess remarkable optical properties that differ dramatically from solid spheres. Another type of nanoparticle, gold nanoclusters (2–6 nm), has been a topic of recent interest because of its unique size, which may be advantageous in cellular uptake as well as in nuclear targeting, in addition to the unique optical and electrical properties exhibited by gold nanoclusters [26–29]. Despite their small size, these nanoclusters were found to be stable because the thiolate groups form a protective layer around gold clusters, improving their stability and functionality [30,31].

Star polyhedral gold nanocrystals were synthesized recently by colloidal reduction of gold with ascorbic acid in water under ambient conditions [32]. Two distinct classes of star nanocrystals were identified: multiple-twinned crystals with fivefold symmetry and monocrystals. These respective classes correspond to icosahedra and cuboctahedra, two Archimedian solids, with preferential growth of their {111} planes. Due to this preferential growth, the {111} faces of the original Archimedean solids grow to become tetrahedral pyramids, the base of each pyramid being the original polyhedral face. By assuming a star morphology, gold nanocrystals increase in proportion to the exposed {111} planes and have low surface energy that could be highly useful for creating stable and biologically active surfaces. Gold nanostars exhibit high plasmonic resonance due to juxtapositioning of the tips that radially emerge from the core making these structures useful for imaging by dark field microscopy, SERS and plasmonics [33–37].

Gold nanocages also represent a unique design in the field of nanomaterials for biology and medicine [38–42]. Gold nanocages with porous walls can be formed using simple galvanic replacement reaction in an electrochemical bath between solutions containing metal precursor salts and silver nanostructures prepared through polyol reduction. The electrochemical potential difference drives the reaction with gold reduction depositing on the surface of the silver nanocubes. Typically, $HAuCl_4$ is used as a metal precursor, the resultant gold is deposited epitaxially on the surface of the silver nanocubes, adopting their underlying cubic form. Concurrent with this deposition, the interior silver is oxidized and removed, together with alloying and de-alloying to produce hollow and eventually, porous structures that are commonly referred to as gold nanocages. By controlling the molar ratio of silver to $HAuCl_4$, the extinction peak of the resultant nanostructures can be continuously tuned from the blue (400 nm) to the NIR (1200 nm) region of the electromagnetic spectrum (FIGURE 3). Calculations suggest that the magnitudes of both scattering and absorption cross-sections of nanocages can be tailored by controlling their dimensions, as well as the thickness and porosity of their walls. This novel class of hollow nanostructures is expected to find use as both a contrast agent for optical imaging in early-stage tumor detection and as a therapeutic agent for photothermal cancer treatment [43–45].

Newer shapes and morphologies of nanoprobes and multifunctional composite nanostructures are being researched. The future of nanoprobe synthesis lies in creative techniques for combining the geometries of two or more probes to enable sharp tuning of optical properties and effective targeted therapy. For example, one could imagine nanorods with needle- shaped structures along the longitudinal axis with surface plasmon bands at lower energies, for use as SERS probes, and in SPR imaging, drug delivery and photothermal/RF therapy. The use of gold with other materials, namely magnetic and polymeric materials, to create new morphologies for imaging and therapy needs to be further investigated to make it cost effective for simultaneous imaging and therapy. However, the creation of new morphologies are only justified if the new materials produce surface plasmon bands at lower energies, enable sensitive colorimetric contrast for imaging, can be utilized as improved SERS probes or have useful photothermal effects for therapy. Finally, the mass production of different types of nanoprobes and their impact on the environment needs to be thoroughly investigated.

## Surface plasmon resonance for optical imaging

Surface plasmon resonance constitutes the collective oscillation of electrons that may exist at the interface of two mediums with dielectric

constants of opposite signs, for instance, a metal and a dielectric [46,47]. The propagation constant of the surface plasma wave propagating at the interface between a dielectric and metal is given by the following expression:

$$\beta = k\left(\varepsilon m \eta s^2 / \varepsilon m + \eta s^2\right)^{1/2}$$

where k denotes the wave number, $e_m = e_{mr} + i_{emi}$ is the dielectric constant of metal and ηs is the refractive index of the dielectric. A material may propagate surface plasmon waves provided, $e_{mr}$ is $<-\eta s^2$. The most common metals that support this condition at optical wavelengths are gold and silver. Nanoprobes of gold and silver scatter light intensely in the visible and NIR region of the electromagnetic spectrum depending upon the size, shape and aggregation of the particles and distance between particulate islands. The scattering of light by nanoparticles is explained by the Mie scattering theory [48] and Maxwell-Garnett theory [49]. The Mie-Gans theory is the extension of Mie's theory for gold particles for particle size much smaller than the excitation wavelength [50]. Depending on the particle size, aggregation and shape, gold nanoparticles in a medium can appear as red, blue or violet in color, thus providing colorimetric contrast (Figure 4). The color scattering property can be useful in biological and cellular applications due to surface functionalization of the particles with appropriate moieties for labeling studies with a white light source and an inexpensive light microscope [51]. Gold nanoparticles in the size range commonly employed (~40 nm) show an absorption cross-section five orders of magnitude larger than conventional absorbing dyes, while the magnitude of light scattering by approximately 80 nm gold nanospheres is five orders higher than the light emission from strongly fluorescing dyes [52]. Table 1 presents the

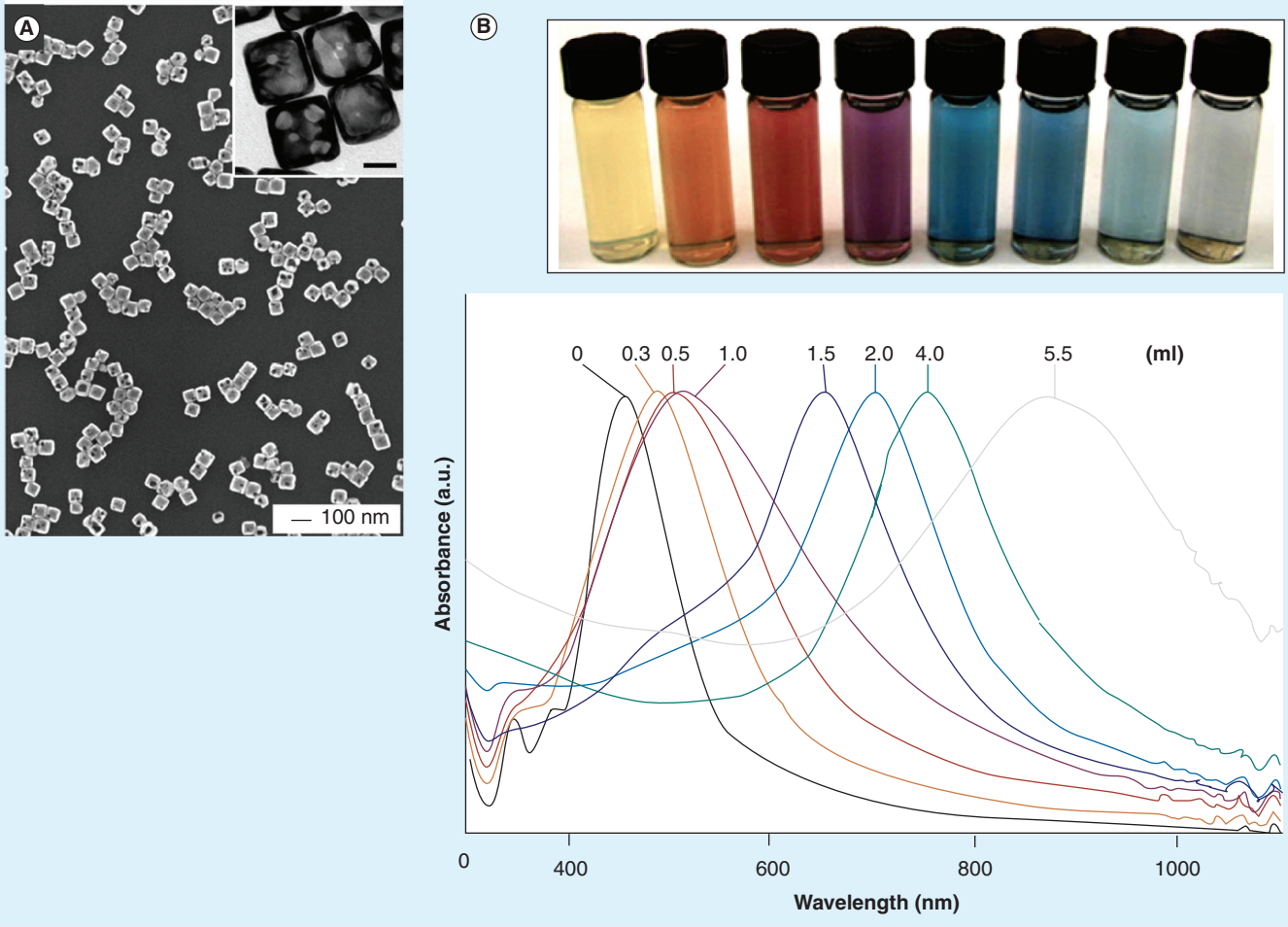


**Figure 4. Colorimetric contrast of nanoprobes. (A)** Transmission electron microscopy image of gold nanocages. **(B)** Colorimetric contrast of silver nanocubes and gold nanocages and their optical absorbance versus wavelength. Gold nanocages prepared by reacting 5 ml of a ~0.2 nM silver nanocube (edge length ~40 nm) suspension with different volumes of a 0.1 mM $HAuCl_4$ solution. The corresponding UV-visible absorbance spectra of silver nanocubes and gold nanocages.
Reproduced with permission from [42].

optical properties of different nanoprobes and compares it with conventional organic dyes generally used for biological imaging.

The metal nanoshells are interesting nanoprobes, because of their silicon dioxide dielectric core and a gold shell. Due to the higher concentration of the electric field in the dielectric core, the propagation constant is highly sensitive to variation in the optical properties of the dielectric adjacent to the metal layer. Variation in the thickness of the metal layer and the dielectric layer can produce a shift in the frequency of the surface plasmon resonance, thereby producing unique colors of metal nanoshells in the visible and near infra-red region of the electromagnetic spectrum. For example, the conventional NIR dye indocyanine green has an absorption cross-section of approximately $10^{-20}$ $m^2$ at approximately 800 nm while the cross-section of the absorbing nanoshells is approximately $4 \times 10^{-14}$ $m^2$, an approximately million-fold increase in absorption cross-section [53].

GNRs possess, in addition to the surface plasmon band around 528 nm seen in gold nanospheres, a band at longer wavelengths due to the plasmon oscillation of electrons along the long axis of the nanorods. Thus, the mode corresponding to the plasmon maximum of the nanorods lies in the desirable NIR region, thus making GNRs potentially useful for *in vivo* applications as NIR radiation is benign to normal cells and tissues. The magnitude of the NIR absorption and scattering ($C_{abs} = 1.97 \times 10^{-14}$ $m^2$ and $C_{sca} = 1.07 \times 10^{-14}$ $m^2$ and at $\lambda = 842$ nm) of nanorods with $r_{eff} = 21.86$ nm is comparable to that of nanospheres and nanoshells, at a much smaller size or volume [52].

Gold nanocages have displayed surface plasmon resonance peaks around 800 nm, a wavelength commonly used in optical coherence tomography (OCT) imaging [39]. OCT measurements on tissue samples embedded with nanoprobes indicate that these gold nanocages have a moderate scattering cross-section of approximately $8.10 \times 10^{-16}$ $m^2$ but a very large absorption cross-section of approximately $7.26 \times 10^{-15}$ $m^2$, suggesting their potential use as a new class of contrast agents for optical imaging [39].

Gold nanostars [35–37] exhibit a short wavelength plasmon band (nanostar core) in the mid-visible region and a long-wavelength plasmon band (nanostar arms), which appears following nucleation and evolves over time in the NIR region [35]. The short and long plasmon peaks are attributed to the plasmon modes associated with the inner core and branch tips, respectively. An interesting aspect of the gold nanostar geometry is the shifting of plasmon resonance with an increase in the size of the star. As the star size increases the short plasmon band centered around 550 nm, usually assigned to the plasmon band of spherical particles, becomes increasingly red-shifted as the spherical core diameter increases in size from 27 to 57 nm. At the same time, the long plasmon band, associated with the rod-like star branches, also undergoes a red shift due to lengthening of branches as well as an overall increase in star size. Due to the sharp nature of the branching tips, gold nanostars could be used as E-field enhancers with the enhancement primarily near the sharp edges and corners. The local surface plasmons oscillating in the direction of the branch and confined at the tips would mainly be excited by components of the incident E-field in the same direction. It is therefore anticipated that the tips would exhibit varying enhancements for any given excitation snapshot taken at 633 nm. Initial studies on SERS signal showed that nanostars exhibited significant enhancement in SERS intensity. As the diameter of nanostar increased from 45 to 116 nm, the SERS enhancement factors increase from $2.0 \times 10^3$ to $3.63 \times 10^3$ [35]. While the reported SERS enhancement factors are averaged over the entire star, significant E-field enhancement could be attained in theory by increasing the number of tips, and reducing the size of the core and its flatness. The nanostar E-field enhancement, and thus SERS efficiency, originate from an intricate interplay of star size, spectral overlap between surface plasmon peaks, excitation wavelength, the number of branches per star surface area, branch aspect ratio, branch length and general star morphology [35]. Further investigation is needed to elucidate the dependence of the physical factors on the plasmon resonance and the associated Raman signal enhancement. The choice of GNPs for biological imaging depends on the application and the expected response, optical resonance wavelength, the extinction cross-section, and the relative contribution of scattering to the extinction with changes in the nanoparticle dimensions.

## Gold nanoprobe-based diagnostics

### Sensors

Diagnostic techniques based on gold nanoparticles involve *in vitro* sensors to detect polynucleotide or proteins [54–58]. In these assays, GNPs are capped with appropriate surface moieties to target oligonucleotides or proteins followed by characterization, which can be conducted by

such methods as atomic force microscopy, scanning electron microscopy, Raman Spectroscopy and other techniques [59–63]. Sub-attomolar concentrations of oligonucleotides have been detected using complementary oligonucleotide-capped gold nanoparticles via high-resolution surface plasmon resonance with signal amplification [64]. This method has been extended to determine p53 cDNA, a polynucleotide tumor suppressor responsible for cellular apoptosis that is frequently mutated in cancer. In this study, the SPR signal changes were reported to be dependent on the p53 cDNA concentration. For target p53 cDNA concentrations of 100 and 300 fM, the corresponding net reported SPR angular shifts were found to be 0.0018 and 0.0030°, respectively. p53 protein dysfunction is associated with poor prognosis and could be used as a molecular indicator for understanding the pathology of the disease and progression [65]. Gold nanoparticles were modified with detector monoclonal antibody and horseradish peroxidase (for signal amplification). The presence of target protein p53 causes the formation of the sandwich structures (magnetic beads–target protein–AuNP probes) through the interaction between the antibodies and the antigen p53. The horseradish peroxidase at the surface of AuNPs catalytically oxidized the substrate to generate optical signals with a sensitivity level of 5 pg $ml^{-1}$ in less than 2 h. The study compared these results to the common antibody–antigen biochemical method known as ELISA, which has a sensitivity of 0.125 ng/assay for p53 [65]. In another recently reported study on GNP sensitivity, an oligonucleotide derived from the human p53 gene with a one-base substitution was distinguished from oligonucelotide with wild-type sequences by a colorimetric change of the GNP solution with a change in pH [66]. All these reports are positive indicators of gold nanoparticles in future disease diagnosis because of their unique physical properties and improvement over conventional methods.

## Imaging

Compared with existing imaging techniques, optical imaging using GNPs is relatively simple. Nanoparticles are intense light scattering agents and therefore simple dark field optical imaging could in principle be used to provide color contrast to image cells tagged by bioconjugated GNPs. The application of gold bioconjugates as contrast agents for vital imaging of precancers was demonstrated with cancer cell suspensions, 3D cell cultures, and normal and neoplastic fresh cervical biopsies [67]. It was demonstrated that gold conjugates can be delivered topically for imaging throughout the whole epithelium. These contrast agents have the potential to extend the ability of vital reflectance microscopy for *in vivo* molecular imaging.

Nanoshells have been used as color contrast agents to target Her2 (human epidermal growth factor receptor associated with breast cancer) in SK-BR-3 cells [25,68,69]. A significant increase in optical contrast under dark field conditions caused by Her2 expression was observed in Her2-positive cells targeted with anti-Her2-labeled nanoshells compared with cells targeted by either anti-IgG-labeled nanoshells or cells not exposed to nanoshell conjugates. Nanoshells are also optimal candidates for OCT. OCT has been performed using gold nanoshells at 1310 nm in water and turbid tissue-simulating phantoms to which nanoshells were added. A monotonic increase in signal intensity and attenuation with increasing shell and core size was observed. Threshold concentrations for a 2-dB OCT signal intensity gain were determined for several nanoshell geometries. For the nanoshell with the largest backscatter (a nanoshell with a 291 nm core diameter and 25 nm shell thickness) a concentration of $10^9$ nanoshells/ml was necessary to produce this signal increase.

GNRs conjugated with an antibody to the EGF receptor have been used to target cancer cells overexpressing Her2. Dark field images were obtained by utilizing nanoparticle scattering. After imaging, photothermal damage was induced by laser excitation of the nanoparticles [51]. This work provided a method for detecting malignant and nonmalignant cells while simultaneously providing a route for targeted therapy by photothermal ablation. In a parallel study, GNRs of different aspect ratios were used to detect multiple cell surface markers on cancer stem cells [70–74]. Cancer stem cells are cells responsible for the initiation and progression of malignant tumors [38,39]. Detection of three cell surface markers frequently expressed on cancer stem cells, CD44, CD42 and CD49f, was possible using dark field spectroscopy and this was validated by flow cytometry [75]. These studies demonstrate the utility and advantages of gold nanoparticles in molecular cancer imaging.

Gold nanoparticles have also found a place as contrast agents in optoacoustic tomography (OAT) [76,77]. OAT is a novel medical imaging method that uses optical illumination and ultrasonic detection to produce deep tissue images based on light absorption. For example,

abnormal angiogenesis in advanced tumors, which increases the blood content of the tumor, is an endogenous contrast agent for OAT. Due to their strong optoacoustic signal, gold nanoparticles (NPs) are also excellent as contrast agents. To target NPs to specific breast cancer cells, the anti-Her2/neu antibody was utilized. Anti-Her2/neu specifically binds cell surface receptors on SK-BR-3 cells. In a series of *in vitro* experiments, Herceptin® (a monoclonal antibody that binds to HER2/neu) conjugated to 40 nm NPs (mAb/NPs) selectively targeted human SK-BR-3 breast cancer cells. The breast cancer cells were detected and imaged by OAT in a gelatin phantom that optically resembled breast tissue. Sensitivity experiments show that a concentration as low as $10^9$ NPs/ml were detectable at a depth of 6 cm, demonstrating its feasibility in deep tissue imaging of solid tumors [76,77]. Recently, drug-loaded aptamer–gold nanoparticle conjugates have been used with CT imaging and therapy of prostate cancer in cell cultures [78]. The resulting prostate-specific membrane antigen aptamer-conjugated GNP showed more than fourfold greater CT intensity for a targeted LNCaP cell (an androgen-sensitive prostate cancer cell) than that of nontargeted PC3 prostate cancer cells. Furthermore, after loading the prostate-specific membrane antigen aptamer-conjugated GNPs with doxorubicin, the GNPs were significantly more potent to the targeted LNCaP cells than against nontargeted PC3 cells.

The inherent luminescence properties of noble metal nanoparticles have been exploited for biosensing and imaging [79–86]. Photoluminescence from noble metals was first reported in 1969 and later observed as a broad background in SERS [87]. In single photon luminescence of metals, excitation of electrons from the d-band to the sp-band to generate electron–hole pairs takes place. The electrons and holes are then scattered on the picosecond time scale with partial energy transfer to the phonon lattice, and finally recombination of electrons and holes resulting in photon emission. Two-photon luminescence (TPL) was described by Boyd *et al.*, and is considered to be produced by a similar mechanism as single photon luminescence but with relatively weak signals [88]. The weak TPL signals can be amplified by several orders of magnitude if they are produced from roughened metal substrates, thereby opening up a new area of GNPs for two photon imaging [88]. Plasmon resonant TPL is attractive for nonlinear optical imaging of biological samples with 3D spatial resolution. GNRs are particularly appealing as TPL substrates because their longitudinal plasmon modes are resonant at NIR, where the absorption of water and biological molecule is minimized [89–91]. Moreover, nanorods have larger local field enhancement factors than nanoparticles due to their reduced plasmon damping [89]. The TPL signal from a single nanorod was shown to be 58-times larger than the two-photon fluorescence signal from a single rhodamine molecule [89]. TPL imaging using GNRs was first used to image single nanorods flowing inside a mouse blood vessel (**Figure 5**) [89]. Following this study, GNRs were used as contrast agents in TPL imaging of cancer cells in 3D tissue phantoms 75 mm deep. The TPL intensity from gold-nanorod-labeled cancer cells was three orders of magnitude brighter than the two-photon autofluorescence emission intensity from unlabeled cancer cells at 760 nm excitation. Other studies using GNRs in two photon imaging have shown the utility of nanorods in imaging [92–95]. The rough star-shaped geometry of gold nanostars could also be highly useful in TPL studies. Studies incorporating magnetic particles with gold have exploited the multifunctional features constituting MRI and photoluminescence imaging [96–99]. Approaches to develop multifunctional nanostructures with multimodal functionalities (e.g., in dual imaging, dual therapy, or targeting and therapy) will have significant implications if they are tailored to treat a specific disease condition. However, such advances focusing on specific applications will require the needed support mechanism from funding agencies and clinicians.

Ultra-sensitive Raman measurements in single living cells were demonstrated by exploiting the SERS [100,101]. Colloidal gold particles (60 nm in size) that are deposited inside cells as 'SERS-active nanostructures' resulted in strongly enhanced Raman signals of the native chemical constituents of the cells [102–109]. Particularly strong field enhancement was observed when gold colloidal particles formed colloidal clusters. The strongly enhanced Raman signals allow Raman measurements of a single cell in the 400–1800 $cm^{-1}$ range with a 1 µm lateral resolution in relatively short collection times (1 s for one mapping point) using 3–5 mW NIR excitation. SERS mapping over a cell monolayer with 1 µm lateral resolution shows different Raman spectra at almost all places, reflecting the inhomogeneous chemical constitution of the cells. Intracellular detection and imaging of multiple SERS probes in zebrafish [110] and multiple metals in single bacterium [111] are other noteworthy efforts in gold nanoparticle-based detection.

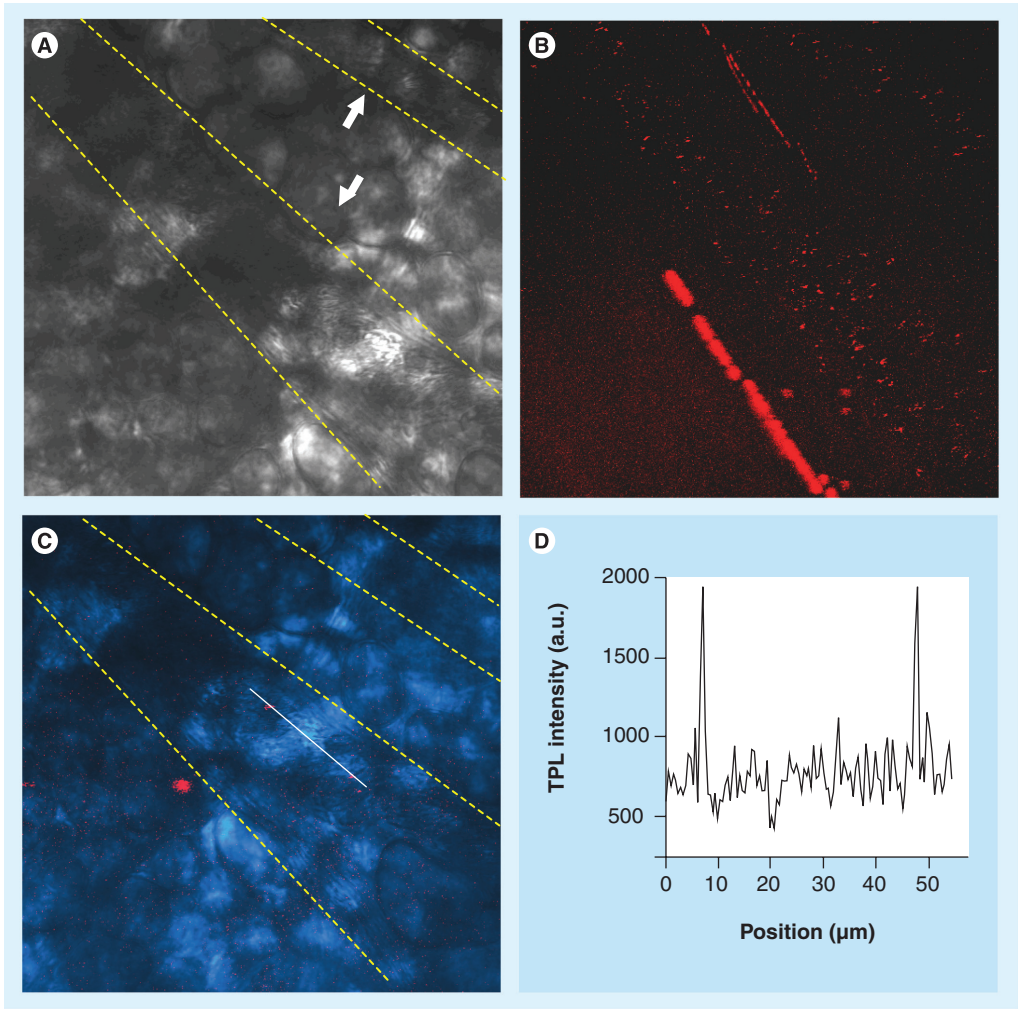


**Figure 5. *In vivo* imaging of single gold nanorods in mouse ear blood vessels.**
**(A)** Transmission image with the two blood vessels indicated. Dotted contour lines are provided to guide the eye. **(B)** TPL image of gold nanorods (red dots) flowing through the blood vessels. Image was compiled as a stack of 300 frames collected continuously at a rate of 1.12 s per frame. The excitation power at the sample was 18 mW with an excitation wavelength of 830 nm; image size is 175 × 175 μm. The bright signal beneath the lower blood vessel is the autofluorescence from a hair root. The streaking is due to sample drift during imaging. **(C)** Overlay of the transmission image (light blue) and a single-frame TPL image. Two single nanorods (red spots) are superimposed by a linescan (white). **(D)** TPL intensity profile from the linescan in **(C)**. The background (~750 a.u.) is due to autofluorescence from the blood vessel and the surrounding tissue. The similar intensities of the red spots indicate the detection of single nanorods.
Reproduced with permission from [89].

Gold nanostars constitute a class of nanoparticles that have been recently shown to be useful SERS probes. Recently measured SERS enhancement factors suggest an interesting correlation between the size of the nanostar (52–116 nm) and SERS efficiencies, which were found to be relatively consistent across different star samples, with an enhancement factor estimated as $5 \times 10^3$ averaged over the 52 nm nanostars for excitation 633 nm [35]. Nanostars could be quite interesting as nanotags as each arm of the star could be used as a plasmonic transducer for sensing biomolecules [112,113].

In summary, GNPs are excellent candidates for biological sensing and medical imaging applications. Their strong signal, resistance to photobleaching, chemical stability, ease of synthesis, simplicity of conjugation chemistry and biocompatibility make GNPs an attractive contrast agent for imaging of cells and tissues. Several types of GNP morphologies are available today to choose from, with tailored functional moieties for molecular imaging. Exploiting gold nanoprobes with conventional techniques such as MRI, CT and OCT will enable selective molecular imaging of targeted cells and tissues

*in vivo* with higher selectivity using appropriate morphologies. Appropriate *in vivo* imaging depends on the optical absorption or scattering properties in specific wavelength windows, targeting surface functional moieties (e.g., Ex: IGF1R, Her2, EpCAM and EGFR), and imaging modalities with sufficient resolution approaching the single cell level. Particles from hybrid metallic materials, such as gold, silver and iron, conjugated with polymer systems can provide for multiple functionalities for multimodal therapeutics. Opportunities in these areas exist and can be exploited further through pathology-based engineering solutions that can only be developed through interactions between engineers, scientists and clinicians.

## Photothermal therapy

Unlike conventional pharmacological approaches (Block Buster Model) towards therapy, nanoprobes are utilized as molecular targeting agents in combination with photothermal vectors for selective killing of cancer cells. By using specific surface moieties that can target diseased cells followed by heating the nanoprobes with NIR light, selective killing of cancer cells and tissues can be achieved in principle without destroying the surrounding normal and healthy cells and tissues. This could translate into minimally invasive treatment options and also prevent the devastating side effects of conventional methods such as chemotherapy and radiation therapy. These methods also have future applications in personalized medicine, which is the idea of treating an individual, not just the disease. In the case of targeted nanoparticles, personalized medicine would entail determining the surface molecules or receptors present on an individual's diseased cells and using these markers to specifically target those individual cells.

The heating effect on light absorption in GNPs is a result of the electron dynamics in metallic lattices [114–118]. Several effects can occur when gold nanoparticles are irradiated with light; these are surface scattering of electrons, electron–phonon coupling and electron–electron thermalization. Due to the high electron density in metals, electron–electron interactions are strong enough to thermalize the electron gas within the duration of the exciting laser pulse. When light is radiated on the metallic nanoparticles, the electrons absorb the photon energy, leading to a nonequilibrium temperature difference between the electron gas and the lattice directly after the laser pulse. Electron–phonon collisions then give rise to the excitation energy exchange between the electron subsystem and the lattice, thereby enabling a thermal equilibrium. Studies on the electron dynamics of gold nanoparticles and nanorods were studied by El Sayed *et al.,* using femtosecond spectroscopy [119]. In their studies a kinetic trace recorded at 530 nm after excitation with 800 nm femtosecond laser pulses produced deviations in the signal intensity versus time profile at an early stage suggesting a finite electron–electron thermalization event, as opposed to phonon–phonon interactions, which would have produced a straight line without any deviations [119]. They also studied the effect of size and shape of the nanoparticles on electron-phonon relaxation. The measured electron–phonon relaxation times were independent of particle size and shape for gold in the investigated size range of 15–48 nm, eliminating the influence of electron-surface scattering as a dominant energy relaxation pathway. The relaxation dynamics of the excited electrons in a nanoshell of gold sulfide nanoparticles coated with an outer layer of gold were reported by Averitt *et al.,* who found a lifetime of 1.7 ps for nanoshells, similar to the results on pure gold nanoparticles [24]. Similarly, studies in ultra-fast relaxation dynamics of gold nanocages found similar relaxation times [115]. Therefore, GNPs primarily undergo similar excitation of electrons causing lattice heating upon irradiation with a laser with no dependence on the size and shape of the particle.

The small size and the rapid heating ability of GNPs within a very small area are quite attractive for selective heating of cancer cells with an appropriate light source thereby leading to the concept of photothermal therapy. In the first such studies, gold nanoshell-mediated photothermal destruction of cancer cells was demonstrated in an animal model [120]. In this study, near infra-red radiation absorbing nanoshells ($10^9$/ml, 20–50 µl) were injected (~5 mm) into solid tumors (~1 cm) in female severe combined immunodeficient mice. Within 30 min of the injection, tumor sites were exposed to NIR light from a laser (820 nm, 4 W/cm$^2$, 5 mm spot diameter, <6 min). Temperature was monitored via a phase-sensitive, phase-spoiled gradient-echo MRI. Magnetic resonance temperature imaging demonstrated that irreversible tumor damage occurred ($\Delta T = 37.4 \pm 6.6°$ C) within 4–6 min. Controls that were exposed to a saline injection rather than nanoshells experienced significantly reduced average temperatures after exposure to the same NIR light levels ($\Delta T$ <10°C). These average temperatures were obtained at a depth of approximately 2.5 mm

below the surface. Histological examination of nanoshell-treated tumors indicated thermal damage including coagulation, cell shrinkage and loss of nuclear staining. Following this study, nanoshells were also targeted to surface receptors namely Her2, which is a growth factor receptor that is commonly seen in more aggressive breast cancer cells. Then, photothermal ablative therapy was administered to selectively destroy the cancer cells [121]. The advantage of GNP-based approaches as opposed to conventional approaches is the ability to accomplish targeting of tumor tissue at the cellular level by exploiting both size (50–500 nm) and specificity, which is possible via modification with targeting molecules. This ensures minimal damage to surrounding healthy tissue and vital organs. Several groups have demonstrated that GNP internalized cells or GNPs in the vicinity of cancer cells can be irradiated with suitable wavelength laser pulses to generate temperatures of approximately 70–80°C to achieve necrotic cell death due to thermal ablation [122–124]. This observation has been translated *in vivo* using mouse models where nanoshells have targeted tumor tissues passively via the enhanced permeability and retention (EPR) effect, which is a result of transendothelial transport via compromised tight junction formation in tumor tissue leading to 'leaky vasculature' and also the lack of lymphatic drainage at tumor locations [125,126]. Another factor that is important is the dose of GNPs delivered to the tumor tissue. It has been demonstrated that a small difference in the dose of GNPs delivered to cancer cells can make a significant difference in the efficiency of tumor ablation [127]. For prostate cancer cells it was recently determined that an average of approximately 5000 gold nanoshells with peak absorption in the NIR region was needed to achieve tumor cell elimination [128]. In addition to delivery via the EPR effect and thermal ablation of tumor tissue, GNPs can also be functionalized to specifically target tumor cells, deliver antiproliferation or apoptosis drugs or stimuli to control tumor growth, and create chemotactic gradients to attract immune cells, such as monocytes for tumor clearance [129]. As discussed in the section above, the thermal properties of gold nanoparticles are unaltered by changes in size and shape. Therefore, GNPs including nanoparticles, nanoshells, nanorods, nanocages and nanostars have shown the ability to selectively destroy cancer cells by utilizing targeting molecules and NIR heating [74,120,130]. Finally, the optical properties of GNPs have been used to develop microscopy, namely absorption, scattering, polarization and photothermal microscopy [131–135]. Finally, the photothermal properties of nanoparticles could potentially be used as a surgical tool in parts of the body considered inaccessible using traditional surgical methods. Along similar lines, administering targeted therapy by disrupting specific genes or proteins in cells and tissues could lead to a new class of opportunities in therapy. These efforts will require appropriate probe design and careful simulation of the electromagnetic and temperature fields to deliver a specific dose of energy for a desired biological effect.

## RF-mediated therapy

RF-mediated therapy (RFA) is a minimally invasive treatment option for focal malignant diseases and is beneficial to surgery because it can reduce morbidity and mortality, is cost effective, is suitable for real-time image guidance and could be implemented on an outpatient basis. RFA involves the use of high temperatures to heat the tumor tissue and kill the cancer cells with minimal injury to normal tissues [136]. During RFA, a high alternating current of approximately 480 KHz is passed into the tumor through an electrode, which causes ionic agitation and frictional heat production, leading to cell death. RFA is a viable treatment option for inoperable tumors of the liver, lungs and bone.

While gold nanoparticles (5–100 nm in diameter) have been shown to interact with shortwave RF waves to produce heat (~300,000 W/g of gold) [137–141], the plasmon absorption property of gold nanoparticles (which is in the range of 520 to 530 nm) is not effective for photothermal therapy. Recent work by us and others have shown that the photon luminescence property of GNRs, because of their tunable absorbance in the NIR region (600–1200 nm), makes them excellent optical imaging agents as well as efficient and more effective photothermal agents due to their nonisotropy [70,77,89]. Although NIR-mediated ablation has shown promise, the efficacy is limited by treatment options that are practical and capable of treating deep-seated tumors (>2–3 cm deep). However, RF has the potential to overcome the penetration depth issues. Multimaterial nanoparticles (comprising of gold and magnetic particles) will have the potential to be responsive to RF treatment and alternating magnetic frequency, facilitating long-term possibility. When conjugated with tumor targeting agents such as monoclonal antibodies, folate, peptides or aptamers, these dual agents

could be used for simultaneous targeting and multimodal therapy by RF ablation and monitoring by imaging (MRI). If selective ablation could be administered at sites where the concentration of nanoparticles is above a threshold (potentially at a tumor site due to targeting) because of localized enhancement of ablation using low level RFA, then only tumor cells at the tumor site will be killed and the normal cells could potentially be left unaffected or subjected to a dose sufficiently minimal to not induce cytotoxicity. In the past, RF treatments that use macroscopic electrodes tend to be painful due to damage to tissues surrounding the electrodes. However, the use of micro/nanoelectrodes could make this technique less invasive and more effective. Photothermal heating using RF waves could be highly useful for selective killing of cancer cells that are pretargeted using GNPs.

## GNP interactions with biological systems

While the above sections primarily discussed the intrinsic factors namely the synthesis, morphology, optical absorption, surface plasmon resonance and electron thermalization properties of GNPs, in this section, we showcase extrinsic factors for successful application of theranostics using GNPs. Some of them include surface functionalization, prevention of aggregation and targeted delivery. Evaluation of the toxicity of GNPs used *in vivo* is also an important requirement that needs to be evaluated prior to application although most GNPs in the size ranges discussed are considered nontoxic. This section details these issues using examples that may or may not directly pertain to cancer but in general are applicable to theranostics.

### Functionalization, targeting & delivery of GNPs to target cells

GNPs provide unique opportunities to accomplish delivery of targeted therapeutics (i.e., drug or gene delivery to specific locations for cancer treatment). Targeted therapy offers significant advantages over free drugs administered systemically in the form of improved stability, site-specific release and elimination of harmful side effects due to interaction with nontarget tissues. This process, however, is a complex problem and involves design strategies to enable conjugation of the drug or gene to the nanoparticle, targeting to the cells or tissue of interest and controlled release of the drug, while at the same time overcoming issues with transit through the body or nontargeted tissue, nonspecific delivery or biodistribution, and clearance from the system or effects of residual GNPs within the system. Although several of these issues have not been completely addressed, *in vitro* and animal studies using GNPs have shown tremendous potential to enhance drug delivery to target cells and reduce toxicity of the free drug to nontarget organs to result in an overall increase in the 'therapeutic index', an indicator of therapy efficacy.

#### Surface modification of GNPs

The primary purpose of surface modification is the prevention of aggregation and solubilization in aqueous solution. To accomplish this, a suitable ligand molecule needs to be identified to accomplish binding via mechanisms such as chemisorption, electrostatic attraction or hydrophobic interaction to the GNP. In addition to consideration of affinity to the GNP, the interaction of the ligand with the medium of suspension also plays an important role in the selection of an appropriate ligand. Coverage using hydrophobic molecules such as thiols [142–144], amines or phosphines [145], trioctylphosphine oxide [146], triphenylphosphine [147], TOAB [148] and oleic acid [149] have been used to prevent aggregation or precipitation. Synthesis of GNPs is typically accomplished in organic solvents whereas most biological applications require transfer to and solubility in aqueous solvents. In the event that the particle cannot be synthesized with the ligand of interest, phase transfer via mechanisms such as ligand exchange [150], ligand modification [151], additional coating [152], polymer coating [153] or silanization [154] could be done to ensure compatibility and stability in an aqueous environment. Ligands with hydrophilic chains offer solubility in aqueous environments while hydrophobic chains act as a protective capping layer and ensure stability in a wide variety of bioanalytical environments. An extremely common and versatile technique used for surface modification and functionalization is the use of thiols, organosulfur compounds containing a carbon-sulfhydryl group (-C-SH or R-SH) where the R is usually an alkene. Thiols have the unique property of self-assembling on gold and hence GNP surfaces are commercially available in a modified form with several functional groups for immobilization of various biomolecules on GNP surfaces. Weisbecker *et al.* have shown the formation of self-assembled monolayers on gold colloids in 50% ethanol solution in the presence of alkenethiols with positive and neutral functional groups [142]. They demonstrated that chain length and functionality of the terminal

groups are critical variables that significantly affect flocculation of GNP dispersions and suggest that it occurs due to a loss of surface energy on the gold particles. Further, coverage with thiol monolayers also serves to protect the GNPs from etching. Lin *et al.,* used a two-step process to functionalize GNPs with thiols [143]. They first suspended tetrachloroauric acid by trisodium citrate in water. The chloride and citrate physisorbed on GNPs and was first displaced by thioctic acid, which in turn was exchanged with thiols containing the desired functionality in the subsequent step. From a biological standpoint, a critical issue in the design of nanoparticle drug- and gene-delivery carriers is the size of the nanoparticle itself as it is important to avoid accidental clearance. This can occur via several mechanisms including the excretory system, the reticuloendothelial system or the mononuclear phagocytic system. On the other hand, aggregation or agglomeration of particles within the body can also occur at nonspecific locations and pose problems such as inflammation and altered cellular function. A major factor affecting clearance of particles or aggregation within different tissues and organs is the particle size. In addition, surface modification techniques using naturally occurring polymers such as dextran, chitosan, pullulan and surfactants, including sodium oleate and dodecylamine, have also been used to assess distribution, to avoid detection by the host immune system and to minimize immune responses in specific tissues [155]. Several groups have also used polyethylene glycol (PEG) for surface modification to ensure a 'stealth mode' that enables long-term presence in circulation without clearance via inhibition of recognition for clearance through phagocytosis. Akiyama and Niiodome *et al.* demonstrated that grafting of GNRs with PEG prevented nonspecific interactions with plasma proteins and inhibited agglomeration in circulation, while serving to avoid clearance via the reticuloendothelial system [156,157]. They also determined that increasing the density of PEG molecules on the surface of the nanorods improved *in vivo* delivery. In addition to modification with PEG, functionalization with several other biomolecules has also been accomplished. Using mechanisms such as covalent, noncovalent and electrostatic binding various biomolecules, such as avidin [158], biotin [158], biotin-modified with amine [159] and carboxylic groups [160], DNA [161], RNA [162], proteins [163], peptides[164], enzymes [165] and antibodies [166] have been attached to GNPs. Lee *et al.*, [167] modified GNPs with primary amine groups to create intracellular delivery vehicles for therapeutic siRNA. Amine modified GNPs possess a net positive charge and are capable of forming stable polyelectrolyte complexes with negatively charged siRNA–PEG conjugates with cleavable disulfide groups that can be cleaved in the reductive environment of the cytoplasm.

### Targeting & internalization of GNPs

The ability to target and internalize GNPs into cells and the nucleus at preferred sites is an intriguing concept in the treatment of diseases and in understanding the internal workings of cells. A major advantage of GNPs over other types of nanoparticles is the ease of functionalization via self-assembly using thiol chemistry and the commercial availability of various thiol-linked peptides, proteins and antibodies. Functionalization is important not only to target nanoparticles to specific tissues but also to direct internalization to specific locations within cells where the molecular cargo can be released to perform targeted functions. When the circulatory system is used, the vascular endothelium provides an ideal target as endothelial cells at different locations in the body differ greatly in the expression of surface antigens [168,169] and allow for specific localization to different parts of the body. Targeting of tumor tissue within the body has been accomplished without any surface functionalization, rather relying on the leaky vasculature at those locations by exploiting the EPR effect. Demonstrations of specific targeting to tissues and organs such as the lymph node using anti-CD4 [170], liver using heparin coatings [171], endothelial cells and leukocytes using various inflammatory markers [172], and retinal pigment epithelial cells using polylactide [173] have been accomplished. Recently, Choi *et al.*, [174] demonstrated that modification of GNPs with transferrin, a glycoprotein that binds iron strongly but reversibly, can be used to target tumor cells within various tissue. Using tail vein injections of GNPs modified with both transferrin and PEG, they found that the biodistribution of GNPs was independent of transferrin. However, within a particular tissue such as the liver, the number of GNPs in hepatocytes was small whereas the number of GNPs in nonparenchymal cells was significantly higher indicating preferential accumulation in cancer cells.

Uptake and cellular internalization of GNPs is a highly intriguing and complex process that is not yet well understood. Nanoparticles can enter the cells through different routes that may be available to them in parallel and factors that

favor a specific entry route are not well understood. Cellular internalization to the cytoplasm and nucleus have been widely accomplished using cell penetrating peptides including:

- Penetratin™, a patented basic cell-penetrating peptide that enables cellular uptake of various large, hydrophilic cargos [175];
- TAT, derived from a transactivator of transcription, and other cell penetrating peptides [164,175] that contain a high abundance of positively charged amino acids can facilitate the transport of both small and large molecular cargo across cell membranes;
- Anti-actin targeting molecules [176], which have a high affinity for intracellular actin;
- Sweet arrow peptide [177], which acts in ways similar to TAT peptides;
- Nuclear localization sequences that are essentially peptide sequences that target the proteins via the cytosolic nuclear transport receptors or nuclear pore complex;
- Receptor-mediated endocytosis peptides [178] such as clathrin, which is a major component of vesicles and plays a key role in the translocation of vesicles into the cytoplasm via endocytosis.

The binding of transferrin (discussed previously) to its receptor on the cell surface has also been exploited to accomplish intracellular translocation [179]. Gene delivery approaches have used GNPs capped with polyethylenimine [180], a polycationic molecule widely used in DNA transfections due to its ability to interact with negatively charged DNA. Liposomal delivery using vesicles made out of a bilayer of phospholipids to encompass aqueous cargo for intracellular deliver has also been explored [181]. It is now believed that this process occurs due to endocytosis rather than fusion with the cell membrane [182]. Finally, strategies such as microinjection [183] to subcellular locations and ultrasound based sonoporation [184] have been used to transport GNPs into cells. In summary, further investigations are necessary for understanding the pathways available to cells for internalization. The control of such pathways could lead to delivery of drugs at specific sites inside the cells that can alter the fate of the cell.

### Drug & gene delivery using GNPs

GNPs can be used for the delivery of various types of drugs, DNA, RNA, siRNA and proteins. Once the GNPs reach their targeted destination within the body, efficient release of therapeutic agents is necessary for effective therapy. Release can be accomplished via triggers that can be actuated either internally using chemical/biological activation or externally using physical stimulation. Glutathione-mediated release is a commonly used technique that exploits the difference in levels of thiols in the extracellular and intracellular environment. Glutathione is the most abundant thiol species in the cytoplasm and the major reducing agent in cellular biochemical processes, and in the case of GNPs modified with thiol functional groups can cause exchange of thiol groups on the GNPs resulting in release of functional group [185]. Polizzi *et al.* showed that GNPs can also be used to deliver diatomic therapeutic agents such as nitric oxide (NO) [186]. NO plays an important role in the regulation of blood vessel tone and controlled release is important under clinical conditions such as hypertension. Efficient storage and controlled release of NO has been demonstrated via covalent linkage with tiopronin-protected gold nanoclusters to form of acid labile *N*-diazeniumdiolate NO donors to enable storage and release of NO on demand [186]. In another example of molecular therapeutics, Hone *et al.,* [187] show the generated singlet oxygen for photodynamic treatment of cancer by mobilizing the surface of the monolayer protected gold particles with photosensitizers, such as phthalocyanines, which on photoactivation generate singlet oxygen.

GNPs can be used as efficient carriers of DNA molecules. DNA–GNPs have been shown to enter a wide variety of cell types. Transport of DNA molecules is one form of gene therapy where target DNA is introduced directly to the cells' nucleus. Passive targeting has been accomplished by relying on the electrostatic interactions of thiol-linked DNA with GNPs [188], which resist enzymatic degradation [189] and can be released via glutathione in the cytoplasm following charge-based transport of the DNA to the nucleus [190]. Thomas *et al.* used hybrid nanoparticle transfection vectors that were created using functionalized GNPs with branched polyethylenimine and showed highly improved transfection efficiency using a cell culture model [191]. Photochemical release or uncaging of DNA immobilized to the surface of GNPs was demonstrated by Rotello *et al.* by changing the nature of GNPs from cationic to anionic via immobilization of a photocleavable *O*-nitrobenzyl ester linker and a quaternary

ammonium salt end group [192]. Oishi *et al.* accomplished covalent linkage of nucleic acids to GNPs for siRNA delivery by modifying the siRNA with a thiol group for self-assembly to the surface of the particle [193]. Finally, Verma *et al.* used GNPs for the delivery of proteins using various strategies, including complementary electrostatic interactions with the nanoparticle in conjunction with glutathione-mediated release [194]. Chitosan-coated particles strongly adsorb insulin and have been used for cellular delivery of insulin [195].

## Biological toxicity of GNPs

Gold in the macro- or micro-scale is chemically inert and biocompatible. At the nanoscale it is widely accepted that particles larger than 5 nm behave similar to bulk gold whereas at sizes of <5 nm the chemical reactivity of gold is significantly altered [196]. $Au_{55}$ clusters at 1.4 nm diameters exhibited significant toxicity compared with their 18 nm counterpart on most human cancer as well as healthy cell lines [197]. However, the response of cells and biological systems to smaller GNPs is still not fully understood. Over the past few years with the rapid increase in GNP technologies for biomedical applications, several groups have sought to address this critical problem. Prior to the use *in vivo*, it is important to evaluate both acute and long-term effects due to potential interaction of GNPs with tissues, organs, circulation and the respiratory tract. This needs to be accomplished by evaluating the toxic effects of GNPs at various levels of cellular organization. Cellular level studies provide the highest specificity (i.e., the ability to identify molecular mediators and signaling mechanisms in cells); however, their relevance (i.e., translation of results from the cell to higher levels of organization) is poor. Intact tissues and organs provide greater relevance at the cost of lower specificity, whereas patient level studies offer the highest relevance albeit with poor specificity. Extensive evaluation of the various factors that influence biocompatibility and toxicity of GNPs is critical for sustained and safe development of novel enabling nanotechnologies.

### Cellular level studies

Use of GNPs for *in vivo* biomedical applications inevitably results in GNP interaction with cells and tissue in the body where GNPs are exposed to physiological fluids such as blood, saliva, the extracellular matrix and even the cytoplasm of a cell. *In vitro* applications involve interaction with cell culture media and other physiological buffers. Most physiological fluids and buffers are a complex mixture of proteins, ions, electrolytes, amino acids, vitamins and other chemicals such as drugs and antibiotics. Physical interaction of GNPs with the constituents of physiological fluids can change physiochemical properties such as size, aggregation, surface charge and chemical/biological specificity influencing subsequent interaction with cells and tissues. High ionic strength solutions are known to cause GNP aggregation due to electrostatic screening [198]. Adsorption of proteins, particularly plasma proteins in blood, alters the behavior of the nanoparticle, changing the biological specificities and interactions by causing the particle to adopt the properties of the adsorbed shell [199–201]. Protein adsorption has also been found to reverse or change the charge on GNRs from cationic to anionic [202] with the potential to enable new functions such as receptor-mediated endocytosis, enabling cellular internalization [203].

Intracellular drug- and gene-delivery studies require an extensive understanding of the mechanisms of uptake of GNPs into cells, localization within the cell and changes in cellular signaling mechanisms as a consequence of uptake [204,205]. Cells typically accomplish internalization of particles and macromolecules through processes such as phagocytosis (>500 nm) [206,207], pinocytosis and different types of receptor-mediated endocytosis (<500 nm) [206,207]. Receptor-mediated endocytosis is known to be the primary mechanism of cellular internalization of GNPs smaller than 100 nm in size [175,208,209]. Functionalization of GNPs with ligands such as transferrin and clathrin have been used to enable endocytosis [209]. Modification of GNP surface charge and phobicity has also been exploited to enable direct internalization [210]. Once inside the cell, GNPs have been found to remain trapped in vesicles in the cytoplasm [202,205,209,211]. Release into the cytoplasm or transfer to the nucleus requires further modification with biomolecules to enable penetration of the nuclear membrane [175]. However, other groups claim nuclear internalization without specific modifications [196,212].

Overall, *in vitro* studies using cell culture models have generated significant information on intracellular transport of GNPs and cell structure and function, including changes in cell signaling via oxidative stress response pathways [213], impaired proliferation [214], compromised motility [215,216] and apoptosis [217]. However, these studies have provided little knowledge

on toxicity, especially in the context of *in vivo* application. This can be attributed to diversity in the types of cells and cell lines evaluated and the large variability in GNP types, sizes, doses, surface charge, functionalization and targeting molecules. GNP cellular toxicity studies will therefore benefit from standardization of protocols and systematic analysis of gene and protein expression using relevant cellular level models.

### *In vivo* studies

Toxicity of GNPs *in vivo* can result from a variety of interactions of GNPs locally and systemically within the body. In blood GNPs, especially unmodified small diameter nanorods, could potentially initiate clotting or erythrocyte lysis. Small GNPs comparable in size to bacterial antigens or viruses could elicit an immune response causing activation of leukocytes or white blood cells and local and systemic inflammation. Despite significant research towards various applications, this aspect of GNPs has not been extensively evaluated. Inhalation is an important pathway that could lead to harmful effects of GNPs and cause inflammation of the respiratory tract and breathing disorders. Once GNPs enter the system either via the respiratory tract, blood circulation or within various tissues, the presence of GNPs within the body if detected can result in accumulation in different organs responsible for clearance of waste such as the liver, spleen and kidneys. Accumulation of GNPs in various organs without clearance from the system can potentially be a significant hazard as they are highly stable and more resistant to clearance via metabolism or the excretory system, which could result in altered cellular function and/or chronic inflammation due to activation of the host immune system. Therefore, the design of GNPs for *in vivo* biomedical applications requires careful consideration of various factors including size, shape, chemical and biological reactivity in various tissues and within the respiratory and circulatory systems to ensure no adverse reactions occur due to the presence of GNPs *in vivo*.

Relatively few studies have sought to evaluate the direct and indirect effects of GNP interactions in blood. Dobrovolaskia *et al.* examined the immunological response of blood to nanoparticles and found that unmodified GNPs caused lysis of erythrocytes or red blood cells [218]. However, other studies evaluating citrate-modified GNPs smaller than 50 nm in diameter were found to be compatible with blood as they did not induce clotting, platelet aggregation or activation of the complement system [219]. The ability of GNPs to elicit an immune response and cause local and systemic inflammation due to direct interaction with blood or indirectly via presentation by antigen-presenting cells has not been extensively evaluated. However, antigen-bound GNPs have been used to enhance the immune response towards antigens [220]. Studies examining the interaction of GNPs and GNP aggregates in the respiratory tract of mice resulted in increased asthmatic response indicating potential to cause inflammation, signifying the need to exercise caution.

GNP biodistribution studies performed using animal models have provided interesting insights into accumulation of GNPs in various organs and toxicity. Using mice, Hillyer *et al.* showed that size of GNPs (<10 nm) facilitated transport across the gastrointestinal tract indicating the possibility of clearance from the body [221]. De Jong *et al.* extensively evaluated the effect of size on biodistribution using a rat model and tail vein injections [222]. Unmodified 10, 50, 100 and 250 nm GNPs were administered and after 24 h the animals were sacrificed and blood and various organs were collected and analyzed. For all sizes of GNPs, the majority were found in the liver and the spleen. However, clear differences were observed for the 10 nm particles, which were localized in the blood, spleen, liver, testis, lung, and brain whereas other sizes were detected only in the blood, liver and spleen. Sonavane *et al.* [223] performed a similar study in mice using unmodified GNPs 15, 50, 100 and 200 nm. They found similar results to the previous study and also found that 15 and 50 nm particles were able to pass the blood–brain barrier, which has important clinical implications in drug delivery targeting brain tissue. Clearance of GNPs from the body was also found to be size dependent. Large GNPs injected into mice were found to remain even 2 years after *in vivo* delivery [224]. This is thought to be due to the inability of the kidney to filter and clear particles smaller than 6 nm [225]. Most applications use GNPs larger than 6 nm and these particles were found to be removed from blood via the reticuloendothelial system and accumulate in the liver and spleen [222,226]. **Figure 6** presents the histological map of PEGylated gold nanoparticles in different organs, namely muscle (**Figure 6B**), liver (**Figure 6C**) and lungs (**Figure 6D**).

## Conclusion & future perspective

Gold has fascinated human beings since time immemorial and colloidal gold has been known

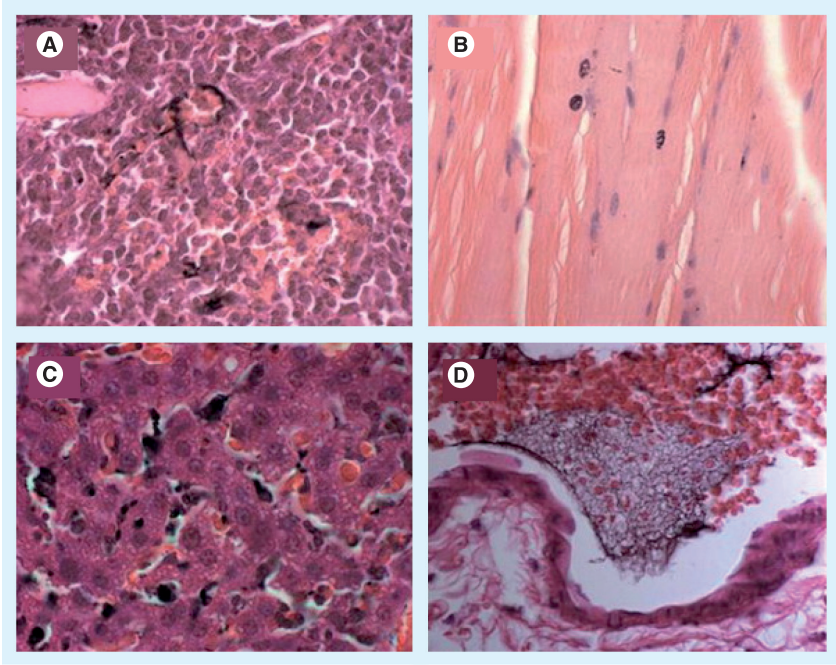


**Figure 6. Histology images (40×) of PEGylated gold particles in different organs 24 h after injection. (A)** Tumor; **(B)** muscle; **(C)** liver; and **(D)** lung. Reproduced with permission from [228].

for centuries. In the past 10 years, there has been tremendous interest in studying the physical properties of different types of GNPs and their optical properties (namely surface plasmon resonance) and investigating their interactions with biological materials. The fundamental interest in GNPs arises due to their enhanced absorption cross-section compared with conventional organic dyes that are also prone to photobleaching effects. The ease of synthesis, chemical stability, wide variety of surface functionalization protocols and the electron thermalization effects resulting in heating has made GNPs prime candidates for future forays in nanomedicine. Cellular level studies show that gold nanoparticles can enter the cells and even the nucleus of cells with simple surface functionalization protocols. These aspects of gold can find applications in *in vitro* diagnostics and in understanding cellular uptake pathways and localization mechanisms. GNPs have been demonstrated as contrast agents in OCT, OAT and CT imaging *in vivo*. The heating effects have been shown to destroy cancer cells in mouse models with the potential to be used in surgery in places that are considered inoperable using conventional surgical methods (e.g., large arteries, veins or the brain).

Several areas of GNPs need further investigation. In the area of synthesis new types of GNP morphologies that combine one or more of the already existing shapes need to be investigated with an intent to create structures with intense and relevant plasmon modes to study the electron transfer process in live cells. The drive towards developing structures with plasmon bands at lower energies, increased absorption and scattering cross-sections, and with calorimetric tunability could be useful in single cell diagnostics. In the area of functionalization, new methodologies and protective coatings that can impart stability in a wide variety of biological environments, enable ease of aqueous solubility and finally prevent aggregation must be investigated. Factors such as nanoparticle size, surface charge, hydrophobic/hydrophilic interactions, and bioaccessibility become highly important for the successful interrogation of cells.

An area that needs critical investigation is the elucidation of nanoparticle uptake pathways, which are still not clear. A better understanding of nanoparticle interaction and uptake could lead to effective targeting for increased treatment efficacy. Although several nanoparticle assays exist, live cell quantification assays have been scarce [70]. Quantification coupled with uptake and internalization studies can provide valuable information on compartmentalized dynamics as well as precise information on localization and drug release.

For the most part, gold is considered nontoxic. However, recent reports show that at particle diameters of less than 5 nm, the surface reactivity of gold increases. $Au_{55}$ clusters with diameters of 1.4 nm have been reported to be toxic in a variety of human cancer as well as healthy cell lines [197]. Therefore, it is vital to conduct long-term studies of its distribution in different cellular organelles and to understand the size and surface modification effects *in vivo*. The ability of GNPs to elicit an immune response and cause local and systemic inflammation due to direct interaction with blood or indirectly via presentation by antigen-presenting cells has not been extensively evaluated. Relatively few studies exist on the direct and indirect interactions of GNPs in blood. Instrumentation that integrates simultaneous imaging and guided therapy with a multimodal functionality in a single step will be attractive for basic studies as well as in clinical applications. While numerous studies exist, a specific and significant application is still lacking. Progress need not necessarily encompass a particle performing multiple functions. A significant step could also follow the notion of "less is more". Despite the advances and obstacles, the future of nanoparticle-based theranostics looks

bright and requires the integration of investigators, especially a clinical or an industry partner early in the research so that practical approaches could be designed to increase impact.


### Financial & competing interests disclosure

*This work was partially supported by NIH R15CA156322 from NCI, NSF CAREER award (ECCS:0853066) and CTSPGSP award at the University of Louisville for B Panchapakesan. The NSF-IDBR-0754740, NIH R21CA157395-01 grants awarded to J Irudayaraj (Co-PI). The Indo-US Knowledge network grant awarded to J Irudayaraj and M Rao, Purdue University Ross fellowship to B Book-Newell and the PCCR (Purdue University) and CTSI (Purdue-IU) awarded to J Irudayaraj. The authors have no other relevant affiliations or financial involvement with any organization or entity with a financial interest in or financial conflict with the subject matter or materials discussed in the manuscript apart from those disclosed.*

*No writing assistance was utilized in the production of this manuscript.*


### Executive summary

- Theranostics describes the fusion of diagnostics and therapeutics for efficient monitoring of personalized response to therapy and better patient care.
- Nanotechnology can be used in theranostics through contrast agents for imaging, immunotargeted therapy, efficient drug delivery and detection.
- Gold nanoprobes (GNPs) are nanovectors of different shapes namely spherical nanoparticles, nanoshells, nanostars, nanocubes and nanocages. They vary in size (between 2 and 500 nm).
- The ability to tune the optical absorption of GNPs through surface plasmon resonance is attractive, and they can be used as coloromiteric and luminescing agents.
- The absorption cross-section of GNPs is about five orders of magnitude larger than conventional fluorescing organic dyes such as rhodamine and indocyanine.
- GNPs are mostly nontoxic and therefore are prime candidates for injectable drug- and gene-delivery vectors.
- The surface functionality of GNPs can be altered through appropriate moieties such as proteins, lipopolysaccharides, DNA and antibodies.
- The electron thermalization state of GNPs upon absorption of light in the near-infared region makes them promising as photothermal agents that can target and selectively kill diseased cells with minimal disruption to the normal cells and tissues.
- Simultaneous imaging and therapy using GNPs with multifunctional properties provides opportunities in multimodal theranostics.

## References


1 Ozdemir V, Williams-Jones B, Glatt SJ, Tsuang MT, Lohr JB, Reist C. Shifting emphasis from pharmacogenomics to theragnostics. *Nat. Biotechnol.* 24, 942–946 (2006).

2 Pene F, Courtine E, Cariou A, Mira JP. Toward theragnostics. *Crit. Care Med.* 37, S50–S58 (2009).

3 Faraday M. Experimental relations of gold (and other metals) to light. *Phil. Trans. Royal Soc. Lond.* 147, 145 (1857).

4 Turkevich J, Stevenson PC, Hillier J. A study of the nucleation and growth processes in the synthesis of colloidal gold. *Faraday Society* 11, 55–75 (1951).

5 Turkevich J, Stevenson PC, Hillier J. The formation of colloidal gold. *J. Phys. Chem.* 57, 670–673 (1953).

6 Turkevich J, Stevenson PC, Hillier J. The color of colloidal gold. *J.Coll. Sci.* 9, 26–35 (1954).

7 Kimling J, Maier M, Okenve B, Kotaidis V, Ballot H, Plech A. Turkevich method for gold nanoparticle synthesis revisited. *J. Phys. Chem. B* 110, 15700–15707 (2006).

8 Uppal MA, Kafizas A, Ewing MB, Parkin IP. The effect of initiation method on the size, monodispersity and shape of gold nanoparticles formed by the Turkevich method. *N. J. Chem.* 34, 2906–2914 (2010).

9 Brust M, Walker M, Bethell D, Schiffrin DJ, Whyman R. Synthesis of thiol-derivatized gold nanoparticles in a 2-phase liquid-liquid system. *J. Chem. Soc. Chem. Comm.* 801–802 (1994).

10 Goulet PJG, Lennox RB. New insights into Brust-Schiffrin metal nanoparticle synthesis. *J. Am. Chem. Soc.* 132, 9582–9584 (2010).

11 Perrault SD, Chan WCW. Synthesis and surface modification of highly monodispersed, spherical gold nanoparticles of 50–200 nm. *J. Am. Chem. Soc.* 131, 17042 (2009).

12 Yu YY, Chang SS, Lee CL, Wang CRC. Gold nanorods: electrochemical synthesis and optical properties. *J. Phys. Chem. B* 101, 6661–6664 (1997).

13 Chen CD, Cheng SF, Chau LK, Wang CRC. Sensing capability of the localized surface plasmon resonance of gold nanorods. *Biosens. Bioelectron.* 22, 926–932 (2007).

14 Chu KC, Chao CY, Chen YF, Wu YC, Chen CC. Electrically controlled surface plasmon resonance frequency of gold nanorods. *Appl. Phys. Lett.* 89, 103–107 (2006).

15 Elim HI, Yang J, Lee JY, Mi J, Ji W. Observation of saturable and reverse-saturable absorption at longitudinal surface plasmon resonance in gold nanorods *Appl. Phys. Lett.* 88, 083107 (2006).

16 Nikoobakht B, Wang JP, MA El-Sayed. Surface-enhanced Raman scattering of molecules adsorbed on gold nanorods: off-surface plasmon resonance condition. *Chem. Phys. Lett.* 366, 17–23 (2002).

17 Johnson CJ, Dujardin E, Davis SA, Murphy CJ, Mann S. Growth and form of gold nanorods prepared by seed-mediated, surfactant-directed synthesis. *J. Mat. Chem.* 12, 1765–1770 (2002).

18 Nikoobakht B, El-Sayed MA. Preparation and growth mechanism of gold nanorods (NRs) using seed-mediated growth method. *Chem. Mat.* 15, 1957–1962 (2003).

19 Gole A, Murphy CJ. Seed-mediated synthesis of gold nanorods: role of the size and nature of the seed. *Chem. Mat.* 16, 3633–3640 (2004).

20 Jana NR, Gearheart L, Murphy CJ. Wet chemical synthesis of high aspect ratio cylindrical gold nanorods. *J. Phys. Chem. B* 105, 4065–4067 (2001).

21 Busbee BD, Obare SO, Murphy CJ. An improved synthesis of high-aspect-ratio gold nanorods. *Adv. Mat.* 15, 414 (2003).

22 Averitt RD, Westcott SL, Halas NJ. Ultrafast optical properties of gold nanoshells. *J. Opt. Soc. Am. B Opt. Phys.* 16, 1814–1823 (1999).

23 Averitt RD, Westcott SL, Halas NJ. Linear optical properties of gold nanoshells. *J. Opt. Soc. Am. B Opt. Phys.* 16, 1824–1832 (1999).

24 Averitt RD, Westcott SL, Halas NJ. Ultrafast electron dynamics in gold nanoshells. *Phys. Rev. B* 58, 10203–10206 (1998).

25 Loo C, Lin A, Hirsch L *et al.* Nanoshell-enabled photonics-based imaging and therapy of cancer. *Technol. Cancer Res. Treat.* 3, 33–40 (2004).

26 Mitchell JW. Nanoclusters of silver and gold atoms. *J. Photographic Sci.* 44, 82–86 (1996).

27 Chan YNC, Schrock RR, Cohen RE. Synthesis of silver and gold nanoclusters within microphase-separated diblock copolymers. *Chem. Mat.* 4, 24–27 (1992).

28 Martino A, Yamanaka SA, Kawola JS, Loy DA. Encapsulation of gold nanoclusters in silica materials via an inverse micelle/sol-gel synthesis. *Chem. Mat.* 9, 423–429 (1997).

29 Mohamed MB, Wang ZL, El-Sayed MA. Temperature-dependent size-controlled nucleation and growth of gold nanoclusters. *J. Phys. Chem. A* 103, 10255–10259 (1999).

30 Garzon IL, Rovira C, Michaelian K *et al.* Do thiols merely passivate gold nanoclusters? *Phys. Rev. Lett.* 85, 5250–5251 (2000).

31 Jin RC. Quantum sized, thiolate-protected gold nanoclusters. *Nanoscale* 2, 343–362 (2010).

32 Burt JL, Elechiguerra JL, Reyes-Gasga J, Montejano-Carrizales JM, Jose-Yacaman M. Beyond Archimedean solids: star polyhedral gold nanocrystals. *J. Crystal Growth* 285, 681–691 (2005).

33 Esenturk EN,Walker ARH. Surface-enhanced Raman scattering spectroscopy via gold nanostars. *J. Raman Spect.* 40, 86–91 (2009).

34 Wu HL, Chen CH, Huang MH. Seed-mediated synthesis of branched gold nanocrystals derived from the side growth of pentagonal bipyramids and the formation of gold nanostars. *Chem. Mat.* 21, 110–114 (2009).

35 Khoury CG, Vo-Dinh T. Gold nanostars for surface-enhanced Raman scattering: synthesis, characterization and optimization. *J. Phys. Chem. C* 112, 18849–18859 (2008).

36 Kumar PS, Pastoriza-Santos I, Rodriguez-Gonzalez B, Garcia de Abajo FJ, Liz Marzan LM. High-yield synthesis and optical response of gold nanostars. *Nanotechnology* 19, 015606 (2008).

37 Krichevski O, Markovich G. Growth of colloidal gold nanostars and nanowires induced by palladium doping. *Langmuir* 23, 1499–1496 (2007).

38 Hu M, Petrova H, Chen JY *et al.* Ultrafast laser studies of the photothermal properties of gold nanocages. *J. Phys. Chem. B* 110, 1520–1524 (2006).

39 Cang H, Sun T, Li ZY *et al.* Gold nanocages as contrast agents for spectroscopic optical coherence tomography. *Optics Lett.* 30, 3048–3050 (2005).

40 Chen JY, Wiley B, Li ZY *et al.* Gold nanocages: engineering their structure for biomedical applications. *Adv. Mater.* 17, 2255–2261 (2005).

41 Chen J, Saeki F, Wiley BJ *et al.* Gold nanocages: bioconjugation and their potential use as optical imaging contrast agents. *Nano Lett.* 5, 473–477 (2005).

42 Skrabalak SE, Chen JY, Sun YG *et al.* Gold nanocages: synthesis, properties, and applications. *Acc. Chem. Res.* 41, 1587–1595 (2008).

43 Cobley CM, Au L, Chen JY, Xia YN. Targeting gold nanocages to cancer cells for photothermal destruction and drug delivery. *Expert Opin. Drug Deliv.* 7, 577–587 (2010).

44 Chen JY, Yang MX, Zhang QA *et al.* Gold nanocages: a novel class of multifunctional nanomaterials for theranostic applications. *Adv. Func. Mat.* 20, 3684–3694 (2010).

45 Rycenga M, Wang ZP, Gordon E *et al.* Probing the photothermal effect of gold-based nanocages with surface-enhanced Raman scattering (SERS). *Angew Chem. Int. Ed. Engl.* 48, 9924–9927 (2009).

46 Homola J, Yee SS, Gauglitz G. Surface plasmon resonance sensors: review. *Sens. Act.s B Chem.* 54, 3–15 (1999).

47 Pattnaik P, Srivastav A. Surface plasmon resonance - applications in food science research: a review. *J. Food Sci. Tech. Mysore* 43, 329–336 (2006).

48 Mie G. Beiträge zur Optik trüber Medien, speziell kolloidaler Metallösungen, Leipzig. *Ann. Physics* 330, 377–445 (1908).

49 Garnett JCM. Colours in metal glasses and in metallic films. *Phil. Trans. Royal Soc. Lond. A* 203, 385–420 (1904).

50 Gans R. Uber die from ultramikroskopischer Goldteilchen. *Ann. Physics* 342, 881–900 (1912).

51 El-Sayed IH, Huang XH, El-Sayed MA. Surface plasmon resonance scattering and absorption of anti-EGFR antibody conjugated gold nanoparticles in cancer diagnostics: applications in oral cancer. *Nano Lett.* 5, 829–834 (2005).

52 Jain PK, Lee KS, El-Sayed IH, El-Sayed MA. Calculated absorption and scattering properties of gold nanoparticles of different size, shape, and composition: applications in biological imaging and biomedicine. *J. Phys. Chem. B* 110, 7238–7248 (2006).

53 Hirsch LR, Stafford RJ, Bankson JA *et al.* Nanoshell-mediated near-infrared thermal therapy of tumors under magnetic resonance guidance. *Proc. Natl Acad. Sci. USA* 100, 13549–13554 (2003).

54 Hazarika P, Ceyhan B, Niemeyer CM. Sensitive detection of proteins using difunctional DNA-gold nanoparticles. *Small* 1, 844–848 (2005).

55 Xia F, Zuo XL, Yang RQ *et al.* Colorimetric detection of DNA, small molecules, proteins, and ions using unmodified gold nanoparticles and conjugated polyelectrolytes. *Proc. Natl Acad. Sci. USA* 107, 10837–10841 (2010).

56 VH Perez-Luna, Aslan K. Interactions of ligand functionalized gold nanoparticles with fluorescently labeled proteins. *Abstracts of Papers of the American Chemical Society* 226, U99–U99 (2003).

57 Abad JM, Mertens SF, Pita M, Fernández VM, Schiffrin DJ. Functionalization of thioctic acid-capped gold nanoparticles for specific immobilization of histidine-tagged proteins. *J. Am. Chem. Soc.* 127, 5689–5694 (2005).

58 Levy R. Peptide-capped gold nanoparticles: towards artificial proteins. *Chem. Bio. Chem.* 7, 1141–1145 (2006).

59 Gearheart LA, Ploehn HJ, Murphy CJ. Oligonucleotide adsorption to gold nanoparticles: a surface-enhanced raman spectroscopy study of intrinsically bent DNA. *J. Phys. Chem. B* 105, 12609–12615 (2001).

60 Zhu ZH, Zhu T, Wang J, Liu ZF. Dependence of the Raman intensity on the surface coverage of nanoparticles in SERS-active gold nanoparticulate films. *Acta Physico Chimica Sinica* 16, 138–144 (2000).

61 Qian LH, Das B, Li Y, Yang ZL. Giant Raman enhancement on nanoporous gold film by conjugating with nanoparticles for single-molecule detection. *J. Mat. Chem.* 20, 6891–6895 (2010).

62 Nguyen CT, Nguyen JT, Rutledge S, Zhang JN, Wang C, Walker GC. Detection of chronic lymphocytic leukemiacell surface markers using surface enhanced Raman scattering gold nanoparticles. *Cancer Lett.* 292, 91–97 (2010).

63 Tong L, Zhu T, Liu Z. Atomic force microscope manipulation of gold

nanoparticles for controlled Raman enhancement. *Appl. Phys. Lett.* 92, 023109 (2008).

64 Yao X, Li X, Toledo F *et al.* Sub-attomole oligonucleotide and p53 cDNA determinations via a high-resolution surface plasmon resonance combined with oligonucleotide-capped gold nanoparticle signal amplification. *Anal. Biochem.* 354, 220–228 (2006).

65 Jia CP, Zhong XQ, Hua B *et al.* Nano-ELISA for highly sensitive protein detection. *Biosens. Bioelect.* 24, 2836–2841 (2009).

66 Sun LP, Zhang ZW, Wang S *et al.* Effect of pH on the interaction of gold nanoparticles with DNA and application in the detection of human p53 gene mutation. *Nano. Res. Lett.* 4, 216–220 (2009).

67 Sokolov K, Follen M, Aaron J *et al.* Real-time vital optical imaging of precancer using anti-epidermal growth factor receptor antibodies conjugated to gold nanoparticles. *Cancer Res.* 63, 1999–2004 (2003).

68 Lin AWH, Lewinski NA, West JL, Halas NJ, Drezek RA. Optically tunable nanoparticle contrast agents for early cancer detection: model-based analysis of gold nanoshells. *J. Biomed. Opt.* 10, 064035 (2005).

69 Agrawal A, Huang S, Wei Haw Lin A *et al.* Quantitative evaluation of optical coherence tomography signal enhancement with gold nanoshells. *J. Biomed. Opt.* 11, 041121 (2006).

70 Chen J, Irudayaraj J. Quantitative investigation of compartmentalized dynamics of ErbB2 targeting gold nanorods in live cells by single molecule spectroscopy. *ACS Nano* 3, 4071–4079 (2009).

71 Yu C, Varghese L, Irudayaraj J. Surface modification of cetyltrimethylammonium bromide-capped gold nanorods to make molecular probes. *Langmuir* 23, 9114–9119 (2007).

72 Yu C, Irudayaraj J. Multiplex biosensor using gold nanorods. *Anal. Chem.* 79, 572–579 (2007).

73 Sun L, Irudayaraj J. PCR-free quantification of multiple splice variants in a cancer gene by surface-enhanced Raman spectroscopy. *J. Phys. Chem. B* 113, 14021–14025 (2009).

74 Wang CG, Chen J, Talavage T, Irudayaraj J. Gold nanorod/$Fe_3O_4$ nanoparticle nano-pearl-necklaces for simultaneous targeting, dual-mode imaging, and photothermal ablation of cancer cells. *Angew. Chem. Int. Ed.* 48, 2759–2763 (2009).

75 Yu CX, Nakshatri H, Irudayaraj J. Identity profiling of cell surface markers by multiplex gold nanorod probes. *Nano Lett.* 7, 2300–2306 (2007).

76 Copland JA, Eghtedari M, Popov VL *et al.* Bioconjugated gold nanoparticles as a molecular based contrast agent: implications for imaging of deep tumors using optoacoustic tomography. *Mol. Imag. Biol.* 6, 341–349 (2004).

77 Taruttis A, Herzog E, Razansky D, Ntziachristos V. Real-time imaging of cardiovascular dynamics and circulating gold nanorods with multispectral optoacoustic tomography. *Optics Express* 18, 19592–19602 (2010).

78 Dhar S, Gu FX, Langer R, Farokhzad OC, Lippard SJ. Targeted delivery of cisplatin to prostate cancer cells by aptamer functionalized Pt(IV) prodrug-PLGA–PEG nanoparticles. *Proc. Natl Acad. Sci. USA* 105(45), 17356–17361 (2008).

79 Nikoobakht B, Burda C, Braun M, Hun M, El-Sayed MA. The quenching of CdSe quantum dots photoluminescence by gold nanoparticles in solution. *Photochem. Photobiol.* 75, 591–597 (2002).

80 Zhu J, Wang YC. Ultraviolet and blue-violet photoluminescence of gold nanoparticles. *Spectros. Spect. Anal.* 2, 235–238 (2005).

81 Lee WI, Bae Y, Bard AJ. Strong blue photoluminescence and ECL from OH-terminated PAMAM dendrimers in the absence of gold nanoparticles. *J. Am. Chem. Soc.* 126, 8358–8359 (2004).

82 Liu L, Zheng HZ, Zhang ZJ, Huang YM, Chen SM, Hu YF. Photoluminescence from water-soluble BSA-protected gold nanoparticles. *Spectrochim. Acta A Mol. Biomol. Spectrosc.* 69, 701–705 (2008).

83 Huang CC, Chiang CK, Lin ZH, Lee KH, Chang HT. Bioconjugated gold nanodots and nanoparticles for protein assays based on photoluminescence quenching. *Anal. Chem.* 80, 1497–504 (2008).

84 Anandan S, Oh SD, Yoon M, Ashokkumar M. Photoluminescence properties of sonochemically synthesized gold nanoparticles for biosensing DNA. *Spectrochim. Acta A Mol. Biomol. Spectrosc.* 76, 191–196 (2010).

85 Nagesha D, Laevsky GS, Lampton P *et al.* *In vitro* imaging of embryonic stem cells using multiphoton luminescence of gold nanoparticles. *Int. J. Nanomed.* 2, 813–819 (2007).

86 Dowling MB, Li LJ, Park J *et al.* Multiphoton-absorption-induced-luminescence (MAIL) imaging of tumor-targeted gold nanoparticles. *Bioconj. Chem.* 21, 1968–1977 (2010).

87 Mooradian A. Photoluminescence of metals. *Phys. Rev. Lett.* 22, 185–187 (1969).

88 Boyd GT, Yu ZH, Shen YR. Photoinduced luminescence from the noble-metals and its enhancement on roughened surfaces. *Phys. Rev. B* 33, 7933–7926 (1986).

89 Wang HF, Huff TB, Zweifel DA *et al.* *In vitro* and *in vivo* two-photon luminescence imaging of single gold nanorods. *Proc. Natl Acad. Sci. USA* 102, 15752–15756 (2005).

90 Imura K, Okamoto H. Properties of photoluminescence from single gold nanorods induced by near-field two-photon excitation. *J. Phys. Chem. C* 113, 11756–11759 (2009).

91 Imura K, Nagahara T, Okamoto H. Near-field two-photon-induced photoluminescence from single gold nanorods and imaging of plasmon modes. *J. Phys. Chem. B* 109, 13214–13220 (2005).

92 He W, Henne WA, Wei QS *et al.* Two-photon luminescence imaging of *Bacillus* spores using peptide-functionalized gold nanorods. *Nano Res.* 1, 450–456 (2008).

93 Tong L, He W, Zhang YS, Zheng W, Cheng JX. Visualizing systemic clearance and cellular level biodistribution of gold nanorods by intrinsic two-photon luminescence. *Langmuir* 25, 12454–12459 (2009).

94 Durr NJ, Larson T, Smith DK, Korgel BA, Sokolov K, Ben-Yakar A. Two-photon luminescence imaging of cancer cells using molecularly targeted gold nanorods. *Nano Lett.* 7, 941–945 (2007).

95 Liaw JW, Tsai SW, Chen KL, Hsu FY. Single-photon and two-photon cellular imagings of gold nanorods and dyes. *J. Nanosci. Nanotech.* 10, 467–473 (2010).

96 Liang GH, Cai SY, Zhang P *et al.* Magnetic relaxation switch and colorimetric detection of thrombin using aptamer-functionalized gold-coated iron oxide nanoparticles. *Anal. Chim. Acta* 689, 243–249 (2011).

97 Kouassi GK, Irudayaraj J. Magnetic and gold-coated magnetic nanoparticles as a DNA sensor. *Anal. Chem.* 78, 3234–3241 (2006).

98 Cho SJ, Jarrett BR, Louie AY, Kauzlarich SM. Gold-coated iron nanoparticles: a novel magnetic resonance agent for T-1 and T-2 weighted imaging. *Nanotechnology* 17, 640–644 (2006).

99 Lin J, Zhou WL, Kumbhar A *et al.* Gold-coated iron (Fe@Au) nanoparticles: Synthesis, characterization, and magnetic field-induced self-assembly. *J. Solid State Chem.* 159, 26–31 (2001).

100 Kneipp J. Nanosensors based on SERS for applications in living cells. *Physics Appl.* 103, 335–349 (2006).

101 Scaffidi JP, Gregas MK, Seewaldt V, Vo-Dinh T. SERS-based plasmonic nanobiosensing in single living cells. *Anal. Bioanal. Chem.* 393, 1135–1141 (2009).

102 Zavaleta CL, Smith BR, Walton I *et al.* Multiplexed imaging of surface enhanced

Raman scattering nanotags in living mice using noninvasive Raman spectroscopy. *Proc. Natl Acad. Sci. USA* 106, 13511–13516 (2009).

103 Benvin AL, Creeger Y, Fisher GW, Ballou B, Waggoner AS, Armitage BA. Fluorescent DNA nanotags: supramolecular fluorescent labels based on intercalating dye arrays assembled on nanostructured DNA templates. *J. Am. Chem. Soc.* 129, 2025–2034 (2007).

104 Martin LC, Larmour IA, Faulds K, Graham D. Turning up the lights-fabrication of brighter SERRS nanotags. *Chem. Comm.* 46, 5247–5249 (2010).

105 Natan MJ. SERS nanotags: a fundamentally new approach to nanoscale optical detection labels. Presented at: *The 231st ACS National Meeting.* Atlanta, GA, USA, 26–30 March, 2006.

106 Ozhalici-Unal H, Armitage BA. Fluorescent DNA nanotags based on a self-assembled DNA tetrahedron. *ACS Nano.* 3, 425–433 (2009).

107 Pallaoro A, Braun GB, Reich NO, Moskovits M. Mapping local pH in live cells using encapsulated fluorescent SERS nanotags. *Small* 6, 618–622 (2010).

108 Xiao M, Nyagilo J, Arora V *et al.* Gold nanotags for combined multi-colored Raman spectroscopy and x-ray computed tomography. *Nanotechnology* 21(3), 035101 (2010).

109 Shamsaie A, Jonczyk M, Sturgi J, Robinson JP, Irudayaraj J. Intracellularly grown gold nanoparticles as potential surface-enhanced Raman scattering probes. *J. Biomed. Opt.* 12(2), 020502 (2007).

110 Wang YL, Seebald JL, Szeto DP, Irudayaraj J. Biocompatibility and biodistribution of surface-enhanced Raman scattering nanoprobes in zebrafish embryos: *in vivo* and multiplex imaging. *ACS Nano.* 4, 4039–4053 (2010).

111 Ravindranath S, Henne K, Thompson D, Irudayaraj J. Surface enhanced Raman imaging of intracellular bioreduction of chromate in shewanella oneidensis. *PLoS ONE* (2011) (In Press).

112 Barbosa S, Agrawal A, Rodriguez-Lorenzo L *et al.* Tuning size and sensing properties in colloidal gold nanostars. *Langmuir* 26, 14943–14950 (2010).

113 Dondapati SK, Sau TK, Hrelescu C, Klar TA, Stefani FD, Feldmann J. Label-free biosensing based on single gold nanostars as plasmonic transducers. *ACS Nano.* 4, 6318–6322 (2010).

114 Link S, Wang ZL, MA El-Sayed. How does a gold nanorod melt? *J. Phys. Chem. B* 104, 7867–7870 (2000).

115 Link S, Burda C, Nikoobakht B, El-Sayed MA. How long does it take to melt a gold nanorod? A femtosecond pump-probe absorption spectroscopic study. *Chem. Phys. Lett.* 315, 12–18 (1999).

116 Mohamed MB, Ismail KZ, Link S, El-Sayed MA. Thermal reshaping of gold nanorods in micelles. *J. Phys. Chem. B* 102, 9370–9374 (1998).

117 Link S, Furube A, Mohamed MB, Asahi T, Masuhara H, El-Sayed MA. Hot electron relaxation dynamics of gold nanoparticles embedded in $MgSO_4$ powder compared with solution: the effect of the surrounding medium. *J. Phys. Chem. B* 106, 945–955 (2002).

118 Mohamed MB, Ahmadi TS, Link S, Braun M, El-Sayed MA. Hotelectron and phonon dynamics of gold nanoparticles embedded in a gel matrix. *Chem. Phys. Lett.* 343, 55–63 (2001).

119 Link S, El-Sayed MA. Shape and size dependence of radiative, non-radiative and photothermal properties of gold nanocrystals. *Int. Rev. Phys. Chem.* 19, 409–453 (2000).

120 Hirsch LR, Stafford RJ, Bankson JA *et al.* Nanoshell-mediated near-infrared thermal therapy of tumors under magnetic resonance guidance. *Proc. Natl Acad. Sci. USA* 100, 13549–13554 (2003).

121 Loo C, Lowery A, Halas N, West J, Drezek R. Immunotargeted nanoshells for integrated cancer imaging and therapy. *Nano Lett.* 5, 709–711 (2005).

122 El-Sayed IE, Huang X, El-Sayed MA. Selective laser photo-thermal therapy of epithelial carcinoma using anti-EGFR antibody conjugated gold nanoparticles. *Cancer Lett.* 239, 129–135 (2006).

123 O'Neal DP, Hirsch LR, Halas NJ *et al.* Photo-thermal tumor ablation in mice using near infrared-absorbing nanoparticles. *Cancer Lett.* 209, 171–176 (2004).

124 Day ES, Morton JG, West LL. Nanoparticles for thermal cancer therapy. *J. Biomech. Eng.* 131, 074001 (2009).

125 Maeda H, Wu J, Sawa T, Matsumura Y, Hori K. Tumor vascular permeability and the EPR effect in macromolecular therapeutics: a review. *J. Control. Release* 65, 271–284 (2000).

126 Iyer AK, Khaled G, Fang J, Maeda H. Exploiting the enhanced permeability and retention effect for tumor targeting. *Drug Disc. Today* 11, 812–818 (2006).

127 Stern JM, Stanfield J, Kabbani W, Hsieh J-T, Cadeddu JA. Selective prostate cancer thermal ablation with laser activated gold nanoshells. *J. Urology* 179, 748–753 (2008).

128 Stern JM, Stanfield J, Lotan Y, Park S, Hsieh J-T, Cadeddu JA. Efficacy of laser-activated gold nanoshells in ablating prostate cancer cells *in vitro*. *J. Endourol.* 21, 939–943 (2007).

129 Wei X-L, Mo Z-H, Li B, Wei J-M. Disruption of HepG2 cell adhesion by gold nanoparticle and paclitaxel disclosed by *in situ* QCM measurement. *Colloids Surfaces B Biointerfaces* 59, 100–104 (2007).

130 Chen JY, Wang DL, Xi JF *et al.* Immuno gold nanocages with tailored optical properties for targeted photothermal destruction of cancer cells. *Nano Lett.* 7, 1318–1322 (2007).

131 Bickford LR, Agollah G, Drezek R, Yu TK. Silica-gold nanoshells as potential intraoperative molecular probes for HER2-overexpression in *ex vivo* breast tissue using near-infrared reflectance confocal microscopy. *Breast Cancer Res. Treat.* 120, 547–555 (2010).

132 Zhou Y, Wu X, Wang T *et al.* A comparison study of detecting gold nanorods in living cells with confocal reflectance microscopy and two-photon fluorescencemicroscopy. *J. Microscopy* 237, 200–207 (2010).

133 Brooke H, Perkins DL, Setlow B, Setlow P, Bronk BV, Myrick ML. Sampling and quantitative analysis of clean *B. subtilis* spores at sub-monolayer coverage by reflectance Fourier transform infrared microscopy using gold-coated filter substrates. *Appl. Spectrosc.* 62, 881–888 (2008).

134 Kim ZH, Leone SR. Polarization-selective mapping of near-field intensity and phase around gold nanoparticles using apertureless near-field microscopy. *Optics Express* 16, 1733–1741 (2008).

135 Bonneau F, Combis P, Rullier JL *et al.* Observation by photothermal microscopy of increased silica absorption in laser damage induced by gold nanoparticles. *Appl. Phys. Lett.* 83, 3855–3857 (2003).

136 Izzo F, Thomas R, Delrio P *et al.* Radiofrequency ablation in patients with primary breast carcinoma – a pilot study in 26 patients. *Cancer* 92, 2036–2044 (2001).

137 Glazer ES, Zhu CH, Massey KL *et al.* Noninvasive radiofrequency field destruction of pancreatic adenocarcinoma xenografts treated with targeted gold nanoparticles. *Clin. Cancer Res.* 16, 5712–5721 (2010).

138 Pedro RN, Thekke-Adiyat T, Goel R *et al.* Use of tumor necrosis factor-alpha-coated gold nanoparticles to enhance radiofrequency ablation in a translational model of renal tumors. *Urology* 76, 494–498 (2010).

139 Cadeddu JA. Use of tumor necrosis factor-alpha-coated gold nanoparticles to enhance radiofrequency ablation in a translational model of renal tumors. *Urology* 76, 494–498 (2010).

140 Moran CH, Wainerdi SM, Cherukuri TK *et al.* Size-dependent Joule heating of gold

nanoparticles using capacitively coupled radiofrequency fields. *Nano Res.* 2, 400–405 (2009).

141 Cardinal J, Klune JR, Chory E *et al.* Noninvasive radiofrequency ablation of cancer targeted by gold nanoparticles. *Surgery* 144, 125–132 (2008).

142 Weisbecker CS, Merritt MV, Whitesides GM. Molecular self-assembly of aliphatic thiols on gold colloids. *Langmuir* 12, 3763–3772 (1996).

143 Lin S-Y, Tsai Y-T, Chen C-C, Lin C-M, Chen C-H. Two-step functionalization ofneutral and positively charged thiols onto citrate-stabilized Au nanoparticles. *J. Phys. Chem. B* 108, 2134–2139 (2004).

144 Love JC, Estroff LA, Kriebel JK, Nuzzo RG, Whitesides GM. Self-assembled monolayers of thiolates on metals as a form of nanotechnology. *Chem. Rev.* 105, 1103–1170 (2005).

145 Leff DV, Brandt L, Heath JR. Synthesis and characterization of hydrophobic, organically-soluble gold nanocrystals functionalized with primary amines. *Langmuir* 12, 4723–4730 (1996).

146 Fleming DA, Williams ME. Size-controlled synthesis of gold nanoparticles via high-temperature reduction. *Langmuir* 20, 3021–3023 (2004).

147 Brown LO, Hutchison JE. Controlled growth of gold nanoparticles during ligand exchange. *J. Am. Chem. Soc.* 121, 882–883 (1999).

148 Thomas KG, Zajicek J, Kamat PV. Surface binding properties of tetraoctylammonium bromide-capped gold nanoparticles. *Langmuir* 18, 3722–3727 (2002).

149 Wang Y, Wong JF, Teng X, Lin XZ, Yang H. Pulling nanoparticles into water: phase transfer of oleic acid stabilized monodisperse nanoparticles into aqueous solutions of αcyclodextrin. *Nano Lett.* 3, 1555–1559 (2003).

150 Kanaras AG, Kamounah FS, Schaumburg K, Kiely CJ, Brust M. Thioalkylated tetraethylene glycol: a new ligand for water soluble monolayer protected gold clusters. *Chem. Comm.* 12(2), 2294–2295 (2002).

151 McMahon JM, Emory SR. Phase transfer of large gold nanoparticles to organic solvents with increased stability. *Langmuir* 23, 1414–1418 (2006).

152 Wooding A, Kilner M, Lambrick DB. Studies of the double surfactant layer stabilization of water-based magnetic fluids. *J. Colloid Interf. Sci.* 144, 236–242 (1991).

153 Wang KT, Iliopoulos I, Audebert R. Viscometric behaviour of hydrophobically modified poly(sodium acrylate). *Polymer Bull.* 20, 577–582 (1988).

154 Mulvaney P, Liz-Marzan LM, Giersig M, Ung T. Silica encapsulation of quantum dots and metal clusters. *J. Mater. Chem.* 10, 1259–1270 (2000).

155 Gupta KA, Gupta M. Synthesis and surface engineering of iron oxide nanoparticles for biomedical applications. *Biomaterials* 26, 3995–4021 (2005).

156 Akiyama Y, Mori T, Katayama Y, Niidome T. The effects of PEG grafting level and injection dose on gold nanorod biodistribution in the tumor-bearing mice. *J. Control. Release* 139, 81–84 (2009).

157 Niidome T, Yamagata M, Okamoto Y *et al.* PEG-modified gold nanorods with a stealth character for *in vivo* applications. *J. Control. Release* 114, 343–347 (2006).

158 Yang W, Wang J, Zhao S, Sun Y, Sun C. Multilayered construction of glucose oxidase and gold nanoparticles on Au electrodes based on layer-by-layer covalent attachment. *Electrochem. Comm.* 8, 665–672 (2006).

159 Kim S, Bawendi MG. Oligomeric ligands for luminescent and stable nanocrystal quantum dots. *J. Am. Chem. Soc.* 125, 14652–14653 (2003).

160 Liu W, Howarth M, Greytak AB *et al.* Compact biocompatible quantum dots functionalized for cellular imaging. *J. Am. Chem. Soc.* 130, 1274–1284 (2008).

161 Yang J, Deivaraj TC, Too H-P, Lee JY. An Alternative phase-transfer method of preparing alkylamine-stabilized platinum nanoparticles. *J. Phys. Chem. B* 108, 2181–2185 (2004).

162 Bowman M-C, Ballard TE, Ackerson CJ, Feldheim DL, Margolis DM, Melander C. Inhibition of HIV fusion with multivalent gold nanoparticles. *J. Am. Chem. Soc.* 130, 6896–6897 (2008).

163 Brewer SH, Glomm WR, Johnson MC, Knag MK, Franzen S. Probing BSA binding to citrate-coated gold nanoparticles and surfaces. *Langmuir* 21, 9303–9307 (2005).

164 de la Fuente JM, Berry CC. Tat peptide as an efficient moleculeto translocate gold nanoparticles into the cell nucleus. *Bioconj. Chem.* 16, 1176–1180 (2005).

165 Zhang S, Wang N, Yu H, Niu Y, Sun C. Covalent attachment of glucose oxidase to an Au electrode modified with gold nanoparticles for use as glucose biosensor. *Bioelectrochemistry* 67, 15–22 (2005).

166 Pissuwan D, Valenzuela SM, Miller CM, Cortie MB. A golden bullet? Selective targeting of *Toxoplasma gondii* tachyzoites using antibody-functionalized gold nanorods. *Nano Lett.* 7, 3808–3812 (2007).

167 Lee SH, Bae KH, Kim SH, Lee KR, Park TG. Amine-functionalized gold nanoparticles as non-cytotoxic and efficient intracellular siRNA delivery carriers. *Int. J. Pharma.* 364, 94–101 (2008).

168 Belloni PN, Nicolson GL. Differential expression of cell surface glycoproteins on various organ-derived microvascular endothelia and endothelial cell cultures. *J. Cell Physiol. Sep.* 136, 398–410 (1988).

169 Rajotte D, Arap W, Hagedorn M, Koivunen E, Pasqualini R, Ruoslahti E. Molecular heterogeneity of the vascular endothelium revealed by *in vivo* phage display. *J. Clin. Invest.* 102, 430–437 (1998).

170 Eck W, Nicholson AI, Zentgraf H, Semmler W, Bartling SN. Anti-CD4-targeted gold nanoparticles induce specific contrast enhancement of peripheral lymph nodes in x-ray computed tomography of live mice. *Nano Lett.* 10, 2318–2322 (2010).

171 Sun I-C, Eun D-K, Na JH *et al.* Heparin-coated gold nanoparticles for liver-specific imaging CT. *Chem. Eur. J.* 15, 13341–13347 (2009).

172 Maurer CA, Friess H, Kretschmann B *et al.* Over-expression of ICAM-1, VCAM-1 and ELAM-1 might influence tumor progression in colorectal cancer. *Int. J. Cancer* 79, 76–81 (1998).

173 Bourges J-L, Gautier SE, Delie F *et al.* Ocular drug delivery targeting the retina and retinal pigment epithelium using polylactide nanoparticles. *Invest. Ophthalmol. Vis. Sci.* 44, 3562–3569 (2003).

174 Choi CHJ, Alabi CA, Webster P, Davis ME. Mechanism of active targeting in solid tumors with transferrin-containing gold nanoparticles. *Proc. Natl Acad. Sci.* 107, 1235–1240 (2010).

175 Nativo P, Prior IA, Brust M. Uptake and intracellular fate of surface-modified gold nanoparticles. *ACS Nano* 2, 1639–1644 (2008).

176 Kumar S, Harrison N, Richards-Kortum R, Sokolov K. Plasmonic nanosensors for imaging intracellular biomarkers in live cells. *Nano Lett.* 7, 1338–1343 (2007).

177 Pujals S, Bastús NG, Pereiro E *et al.* Shuttling gold nanoparticles into tumoral cells with an amphipathic proline-rich peptide. *ChemBioChem.* 10, 1025–1031 (2009).

178 Tkachenko AG, Xie, H, Coleman D *et al.* Multifunctional gold nanoparticle–peptide complexes for nuclear targeting.*J. Am. Chem. Soc. Apr.* 125, 4700–4701 (2003).

179 Yang P-H, Sun X, Chiu J-F, Sun H, He Q-Y. Transferrin-mediated gold nanoparticle cellular uptake. *Bioconj. Chem.*16, 494–496 (2005).

180 Thomas M, Klibanov AM. Non-viral gene therapy: polycation-mediated DNA delivery. *Appl. Microbiol. Biotechnol.* 62, 27–34 (2003).

181 Devika BC, Michael D, James S, Christine A, David AJ. Cellular uptake and transport of gold nanoparticles incorporated in a liposomal carrier. *Nanomedicine* 6, 161–169 (2010).

182 Simões S, Filipe A, Faneca H *et al.* Cationic liposomes for gene delivery. *Exp. Opin. Drug Deliv.* 2, 237–254 (2005).

183 Feldherr CM, Akin D. Signal-mediated nuclear transport in proliferating and growth-arrested BALB/c 3T3 cells. *J. Cell Biol.* 115, 933–939 (1991).

184 Soman N, Marsh J, Lanza G, Wickline S. New mechanisms for non-porative ultrasound stimulation of cargo delivery to cell cytosol with targeted perfluorocarbon nanoparticles. *Nanotechnology* 19, 185102 (2008).

185 Saito G, Swanson JA, Lee K-D. Drug delivery strategy utilizing conjugation via reversible disulfidelinkages: role and site of cellular reducing activities. *Adv. Drug Deliv. Rev.* 55, 199–215 (2003).

186 Polizzi MA, Stasko NA, Schoenfisch MH. Water-soluble nitric oxide-releasing gold nanoparticles. *Langmuir* 23, 4938–4943 (2007).

187 Hone DC, Walker PI, Evans-Gowing R *et al.* Generation of cytotoxic singlet oxygen via phthalocyanine-stabilized gold nanoparticles: a potential delivery vehicle for photodynamic therapy. *Langmuir* 18, 2985–2987 (2002).

188 McIntosh CM, Esposito EA, Boal AK, Simard JM, Martin CT, Rotello VM. Inhibition of DNA transcription using cationic mixed monolayer protected gold clusters. *J. Am. Chem. Soc.* 123, 7626–7629 (2001).

189 Han G, Martin CT, Rotello VM. Stability of gold nanoparticle-bound DNA toward biological, physical, and chemical agents. *Chem. Biol. Drug Design* 6, 78–82 (2006).

190 Han G, Chari NS, Verma A, Hong R, Martin CT, Rotello VM. Controlled recovery of the transcription of nanoparticle-bound DNA by intracellular concentrations of glutathione. *Bioconj. Chem.* 16, 13, 1359–1356 (2005).

191 Thomas M, Klibanov AM. Conjugation to gold nanoparticles enhances polyethylenimine's transfer of plasmid DNA into mammalian cells. *Proc. Natl Acad. Sci. USA* 100, 1938–1943 (2003).

192 Han G, You C-C, Kim B-J *et al.* Light-regulated release of DNA and its delivery to nuclei by means of photolabile gold nanoparticles. *Angew. Chem. Int. Ed.* 45, 3165–3169 (2006).

193 Oishi M, Nakaogami J, Ishii T, Nagasaki Y. Smart PEGylated gold nanoparticles for the cytoplasmic delivery of siRNA to induce enhanced gene silencing. *Chem. Lett.* 35, 1046–1047 (2006).

194 Verma A, Simard JM, Worrall JWE, Rotello VM. Tunable reactivation of nanoparticle-inhibited β-galactosidase by glutathione at intracellular concentrations. *J. Am. Chem. Soc.* 126, 13987–13991 (2004).

195 Bhumkar D, Joshi H, Sastry M, Pokharkar V. Chitosan reduced gold nanoparticles as novel carriers for transmucosal delivery of insulin. *Pharm. Res.* 24, 1415–1426 (2007).

196 Tsoli M, Kuhn H, Brandau W, Esche H, Schmid G. Cellular uptake and toxicity of $Au_{55}$ clusters. *Small* 1, 841–844 (2005).

197 Tsoli M, Kuhn H, Brandau W, Esche H, Schmid G. Cellular uptake and toxicity of AU(55) clusters. *Small* 1, 841–844 (2005).

198 Vesaratchanon S, Nikolov A, Wasan DT. Sedimentation in nano-colloidal dispersions: effects of collective interactions and particle charge. *Adv. Coll. Interf. Sci.* 134–135, 268–278 (2007).

199 Cederval T, Lynch I, Foy M *et al.* Detailed identification of plasma proteins adsorbed on copolymer nanoparticles. *Angew. Chem. Int. Ed.* 46, 5754–5756 (2007).

200 Lynch I,Cedervall T, Lundqvist M *et al.* The nanoparticle-protein complex as a biological entity; a complex fluids and surface science challenge for the 21st century. *Adv. Coll. Interf. Sci.* 13,167–174 (2007).

201 Lynch I, Dawson KA. Protein–nanoparticle interactions. *Nano Today* 3, 40–47 (2008).

202 Alkilany AM, Nagaria PK, Hexel CR, Shaw TJ, Murphy CJ, Wyatt MD. Cellular uptake and cytotoxicity of gold nanorods: molecular origin of cytotoxicity and surface effects. *Small* 5, 701–708 (2009).

203 Conner SD, Schmid SL. Regulated portals of entry into the cell. *Nature* 422, 37–44 (2003).

204 Rosi NL, Giljohann DA,Thaxton CS, Lytton-Jean AKR, Han MS, Mirkin CA. Oligonucleotide-modified gold nanoparticles for intracellular gene regulation. *Science* 312, 1027–1030 (2006).

205 Han G, Ghosh P, Rotello VM. Functionalized gold nanoparticles for drug delivery. *Nanomedicine* 2, 113–123 (2007).

206 Dobrovolskaia MA, McNeil SE. Immunological properties of engineered nanomaterials. *Nat. Nanotechnol.* 2, 469–478 (2007).

207 Hess H, Tseng Y. Active intracellular Transport of nanoparticles: opportunity or threat? *ACS Nano* 1, 390–392 (2007).

208 Shukla R, Bansal V, Chaudhary M, Basu A, Bhonde RR, Sastry M. Biocompatibility of gold nanoparticles and their endocytoticfate inside the cellular compartment: a microscopic overview. *Langmuir* 21, 10644–10654 (2005).

209 Chithrani BD, Chan WCW. Elucidating the Mechanism of cellular uptake and removal of protein-coated gold nanoparticles of different sizes and shapes. *Nano Lett.* 7, 1542–1550 (2007).

210 Verma A, Uzun O, Hu Y *et al.* Surface-structure-regulated cell-membrane penetration by monolayer-protected nanoparticles. *Nat. Mater.* 7, 588–595 (2008).

211 Pernodet N, Fang X, Sun Y *et al.* Adverse effects of citrate/gold nanoparticles on human dermal fibroblasts. *Small* 2, 766–773 (2006).

212 Ryan JA, Overton KW, Speight ME *et al.* Cellular uptake of gold nanoparticles passivated with BSA–SV40 large T antigen conjugates. *Anal. Chem.* 79, 9150–9159 (2007).

213 Thakor AS, Paulmurugan R, Kempen P *et al.* Oxidative stress mediates the effects of raman-active gold nanoparticles in human cells. *Small* 7, 126–136 (2011).

214 Kalishwaralal K, Sheikpranbabu S, BarathManiKanth S, Haribalaganesh R, Ramkumarpandian S, Gurunathan S. Gold nanoparticles inhibit vascular endothelial growth factor-induced angiogenesis and vascular permeability via Src dependent pathway in retinalendothelial cells. *Angiogenesis* 14(1), 29–45 (2010).

215 Baram-Pinto D, Shukla S, Gedanken A, Sarid R. Inhibition of HSV-1 attachment, entry, and cell-to-cell spread by functionalized multivalent gold nanoparticles. *Small* 6, 1044–1050 (2010).

216 Tarantola M, Pietuch A, Schneider D *et al.* Toxicity of gold-nanoparticles: synergistic effects of shape and surface functionalization on micromotility of epithelial cells. *Nanotoxicol.* 5(2), 254–268 (2011).

217 Maiorano G, Sabella S, Sorce B *et al.* Effects of cell culture media on the dynamic formation of protein–nanoparticle complexes and influence on the cellular response. *ACS Nano* 4(12), 7481–7491 (2010).

218 Dobrovolskaia MA, Aggarwal P, Hall JB, McNeil SE. Preclinical studies to understand nanoparticle interaction with the immune system and its potential effects on nanoparticle biodistribution. *Mol. Pharm.* 5, 487–495 (2008).

219 Marina AD, Anil KP, Jiwen Z *et al.* Interaction of colloidal gold nanoparticles with humanblood: effects on particle size and

analysis of plasma protein binding profiles. *Nanomedicine* 5, 106–117 (2009).

220 Bastús NG, Sánchez-Tilló E, Pujals S *et al.* Peptides conjugated to gold nanoparticles induce macrophage activation. *Mol. Immunol.* 46, 743–748 (2009).

221 Hillyer JF, Albrecht RM. Gastrointestinal persorption and tissue distribution of differently sized colloidal gold nanoparticles. *J. Pharm. Sci.* 90, 1927–1936 (2001).

222 De Jong WH, Hagens WI, Krystek P, Burger MC, Sips AJAM, Geertsma RE. Particle size-dependent organ distribution of gold nanoparticles after intravenous administration. *Biomaterials* 29, 1912–1919 (2008).

223 Sonavane G, Tomoda K, Makino K. Biodistribution of colloidal gold nanoparticles after intravenous administration: effect of particle size. *Coll. Surf. B Biointerf.* 66, 274–280 (2008).

224 Ballou B, Ernst LA, Andreko S *et al.* Sentinel lymph node imaging using quantum dots in mouse tumor models. *Bioconj. Chem.* 18, 389–396 (2007).

225 Soo Choi H, Liu W, Misra P *et al.* Renal clearance of quantum dots. *Nat. Biotech.* 25, 1165–1170 (2007).

226 von Maltzahn G, Park JH, Agrawal A *et al.* Computationally guided photothermal tumor therapy using long-circulating gold nanorod antennas. *Cancer Res.* 69, 3892–3900 (2009).

227 Gámez F, Hurtado P, Castillo PM *et al.* UV-vis-NIR laser desorption/ionization of synthetic polymers assisted by gold nanospheres, nanorods and nanostars. *Plasmonics* 5(2), 125–133 (2010).

228 Wang CH, Liu CJ, Chien CC *et al.* X-ray synthesized PEGylated (polyethylene glycol coated) gold nanoparticles in mice strongly accumulate in tumors. *Mater. Chem. Phys.* 126(1–2), 15, 352–356 (2011).